



Fractional Linear Fokker - Planck Equation with Applications

By

Enas Mustafa Nasser Kittaneh

Supervisor

Dr. Basheer Abdallah

Co- Supervisor

Dr. Rami Amro

**This Thesis was submitted in partial fulfillment of the requirements
for the Master's Degree of Science in Mathematical Modeling.**

Faculty of Graduate Studies

Palestine Technical University –Kadoorie.

September 2021



معادلة فوكر بلانك الخطية الكسرية وتطبيقاتها

إعداد

إيناس مصطفى ناصر كتانة

المشرف

د. بشير عبد الله

المشرف المشارك

د. رامي عمرو

قدمت هذه الرسالة استكمالاً لمتطلبات الحصول على درجة الماجستير في النمذجة الرياضية

عمادة البحث العلمي والدراسات العليا

جامعة فلسطين التقنية – خضوري

أيلول 2021

جامعة فلسطين التقنية – خضوري

نموذج التفويض

أنا إيناس مصطفى ناصر كتانة , أفوض جامعة فلسطين التقنية خضوري بتزويد نسخ من رسالتي / أطروحتي للمكتبات والمؤسسات أو الهيئات أو الأشخاص عند طلبهم حسب التعليمات النافذة في الجامعة.

التوقيع :

التاريخ : 2021/ 10/4

PTUK

Authorization form

I , **Enas Mustafa Nasser Kittaneh** , authorize the PTUK University to supply copies of my theises / dissertation to libraries or establishments or individuals on request , according to the University of PTUK regulate

Signature:

Date: 4/ 10 /2021 .

COMMITTEE DECISION

This thesis / dissertation (Fractional Linear Fokker -Planck Equation with Applications).

Examination committee

Signature

Asst. Prof. Basheer Abdallah (supervisor)

Asst. Prof. Rami Amro (Co – supervisor)

Asst. Prof. Raed Al-Masri (External Examiner)

Asst. Prof. Mohammad Marabeh (Internal Examiner)

DEDICATION

After thanking God and my parents' prayers

I dedicate this work to

My dear husband **Nasser** for his constant care and unlimited support

My children (**Meelad, Ghazal, Farah, Adam**)

My brothers

Everyone who gave me advice and help.

ACKNOWLEDGEMENTS

I would like to express my gratitude to all those who helped me to prepare and complete this work, specially to my advisors Dr. Basheer Abdallah, and

Dr. Rami Amro for their help and advice through the period of my study.

Contents

Abstract	xi
Chapter Zero: Introduction	1
Chapter One: Preliminaries.....	6
Chapter Two: Analytic Solution of Fokker-Planck equation.	
2.1: Analytic Solution of Diffusion Equation.....	11
2.2: Analytic Solution of Convection- Diffusion Equation.....	24
2.3: Analytic Solution of Fractional Diffusion Equation.....	32
2.4: Analytic Solution of Fractional Convection -Diffusion Equation.....	39
Chapter Three: Numerical Solution of Fokker-Planck Equation.	
3.1: Explicit Finite Difference Method for Diffusion Equation	42
3.2: Explicit Finite Difference Method for Convection - Diffusion Equation...	52
3.3: Explicit Finite Difference Method for Fractional Diffusion Equation.....	58
3.4 : Explicit Finite Difference Method for Fractional Convection - Diffusion Equation.....	67
Chapter Four: Stochastic Picture of Diffusion Equation.	
4.1 General Treatment	69

4.2 Unbounded Free Diffusion ..	73
4.3 Bounded Free Brownian Motion	82
Conclusion and Outlook	90
References92

List of Figures

2.1.1 Analytic solution of diffusion equation with Dirichlet boundary conditions.....	16
2.1.2 Analytic solution of diffusion equation with Neumann boundary conditions.....	17
2.2.1 Analytic solution of fractional diffusion equation	36
3.1.1 Numerical solution of one dimensional heat equation	49
3.1.2 Numerical solution for Example (3.1.4)	51
3.2.1 Numerical solution of convection-diffusion equation	56
3.3.1 Numerical solution of fractional heat equation.....	64
3.3.2 Numerical solution of fractional diffusion equation with Neumann boundary condition	65
4.2.1 Time traces for unbounded diffusing Brownian particles.....	78
4.2.2 Mean square displacement for Brownian particle.....	80
4.2.3 Normalized probability distribution function	81
4.3.1 Time traces for bounded diffusing Brownian particles.....	85
4.3.2 MSD of reflected Brownian motion in the interval $[0,1]$	86
4.3.3 Different solutions of the FPE for the reflected Brownian motion	87

4.3.4 Probability distribution function for the bounded diffusion case	88
4.3.5 Calculated values of alpha	89

Fractional Linear Fokker -Planck Equation with Applications

ABSTRACT

Fractional calculus is a developing field of research in mathematics. It is used widely in other fields of science and finance with several applications. In this thesis, we solve the linear Fokker -Planck equation (FPE) and fractional Fokker-Planck equation in three different ways: analytically, numerically and stochastically. We solved it for the normal diffusion case and the sub-diffusion case ($0 < \alpha \leq 1$). In the analytical method, the separation of variable technique are used, especially, we discuss the analytical solution in sections 2.2, and 2.4 in details, which was not discussed in details in the previous books and periodicals. In the numerical scheme, we used the explicit finite difference method. In Particular, we investigate the stability of the scheme in section 3.3, which was not discussed in the previous books and periodicals for the approach used in the proof. The stochastic method is used, with help of Euler-Maruyama method, to solve the motion of free diffusing ink molecules in a fluid. Using this method, we solved FPE for the unbounded and bounded case. Unexpectedly, in the bounded case, we noticed the appearance of transient fractional behavior.

المخلص

حساب التفاضل والتكامل الجزئي هو مجال بحث متطور في الرياضيات. يتم استخدامه على نطاق واسع في مجالات أخرى من العلوم والتمويل مع العديد من التطبيقات. في هذه الأطروحة ، قمنا بحل معادلة فوكر بلانك الخطية ومعادلة فوكر بلانك الكسرية بثلاث طرق مختلفة: التحليلية ، العددية والعشوائية.

لقد قمنا بحلها لحالة الانتشار العادية وحالة الانتشار الفرعي ($0 < \alpha \leq 1$) ،

في الطريقة التحليلية تم استخدام تقنية فصل المتغيرات وسوف نناقش الحل التحليلي في القسمين 2.2 و 2.4 بالتفصيل، والذي لم يتم التطرق إليه في الكتب والدوريات السابقة. في الطريقة العددية، استخدمنا طريقة الفروق المحدودة الصريحة. ثم قمنا بالتحري عن استقرار الحل في القسم 3.3، والذي لم تتم مناقشته في الكتب والدوريات السابقة للنهج المستخدم في الإثبات.

تُستخدم الطريقة العشوائية ، بمساعدة طريقة أويلر-ماريوما ، لحل حركة جزيئات الحبر المنتشرة في سائل. باستخدام هذه الطريقة قمنا بحل معادلة فوكر بلانك للحالة غير المحدودة والمحدودة. بشكل غير متوقع في الحالة المحدودة لاحظنا ظهور السلوك الجزئي العابر.

CAPTER ZERO

1) Introduction

Ordinary calculus concerned with derivatives of integer order. The mathematical theory concerned with finding solution for such equations is well developed and extensively used in treating many real world problems. It showed a very profound success in treating problems which are continuously appear in a wide variety of disciplines, such as physics, chemistry, biology and many other contemporary fields. Thus, ordinary calculus is well known and widely used [8; 9]. Hence, describing a dynamical phenomenon with an ordinary differential equation is a normal and can be approached intuitively in many cases just by relating the change of one macroscopic variable with respect of the other. However, a new emerging phenomenon deviates from this way of thinking, and requires more attention, in particular, requires the treatment of differential equation involving non-integer order of the derivative. Such derivatives are called fractional derivatives.

2) Previous studies

Fractional derivatives and fractional calculus found a great attention since the early of the twentieth century, but then it became famous in the second half of the century. Fractional calculus gained this attention due to the rise of many problems in science and finance, more specifically in the diffusion contest, for

elaborate review of the history of fractional calculus and its applications the reader is keenly referred to reference [17].

Fractional calculus succeeded in explaining many experimental observations related diffusion of microscopic organelles in the cell cytoplasm [25; 33; 50], diffusion of charge carriers in semiconductor [12], and in laser physics [18; 23]. Thus, it became a prominent tool that is needed to treat real world problems. While these problems have been extensively and for long though to follow the rules of normal diffusion, where the variance (σ^2) of the microscopic particle position changes linearly with time (t); $\sigma^2 \propto t$. Deviation of the variance from this linear relationship was reported in many experimental observation, and modelled fractional derivatives. Previous studies attributed this behavior of the variance to the existence of obstacles, hindering time [5], motion within confined environment, and various types of constrictions on the particle behavior [10].

Diffusion is a process in which particles initially concentrated around a certain position x_0 in a specific medium, spread away from this position due to the concentration gradient. On the microscopic level, this phenomenon was first reported and explained by Robert Brown (1827) while observing the motion of pollen grains in water. In 1905, Einstein attributed this motion to the random kicks exerted by water molecules on the pollen grain, and was able to relate the mean square displacement to the diffusion coefficient. Later on, this motion

became known as Brownian motion. In 1908, Langevin, formulated a mathematical description of the particle motion which is known today as Langevin picture of the Brownian motion. Langevin view is also a microscopic description relies on the nature of the random force ($\eta(t)$) which he assumed to have a Gaussian distribution centered around zero, meaning that most of these random kicks result in virtually zero force, but few have large value [22; 57].

An alternative view is the macroscopic picture, where instead of following the time evolution of the Brownian particle, one can look to the distribution of the position of many of these particles at specific time instant. This view is formulated using the ergodicity theory where in time averages can be replaced by ensemble averages in the long time limit [47]. Using statistical theory, in 1906 Einstein and Von Smoluchowski explained the physical meaning behind Brown's observations and could calculate the mean squared displacement of the Brownian particles in the stationary state. Around 1927, Fokker and Planck introduced a partial differential equation that show the time evolution of the probability density of the Brownian particle velocity and position [49].

Fractional Fokker-Planck equation (FFPE) is a partial differential equation that involve fractional derivatives in space, time, or both, hence the corresponding FFPE admits the following form

$$\frac{\partial u^\alpha}{\partial t^\alpha} = \left[-d \frac{\partial^\beta}{\partial x^\beta} + c \frac{\partial^{2\beta}}{\partial x^{2\beta}} \right] u(x, t) \quad (1.1.1)$$

We would like to mention that if $\alpha = 1$, $\beta = 1$, then FFPE is called FPE and describes normal diffusion or diffusion with drift if $d \neq 0$, while

If $0 < \alpha < 1$, $\beta = 1$, then FFPE is called sub-diffusion

If $1 < \alpha < 2$, $\beta = 1$, then FFPE is called superdiffusion

If $\alpha = 2$, $\beta = 1$, then FFPE is called ballistic diffusion

Where $\frac{\partial u^\alpha}{\partial t^\alpha}$ is the fractional Caputo or Riemann derivative

where α and β are parameters describing the order of the fractional time and space derivatives, respectively .

In this thesis we will solve one dimensional Fokker-Planck equation in three different methods: analytical, numerically, and stochastically as shown below and we will compare the results for some cases between all methods.

In this thesis , we will consider the following cases for FFPE (1.1.1)

Case1 Part a: Diffusion Equation (when $\alpha = 1$, $\beta = 1$, $d = 0$, c is constant)

Case1 Part b: Convection - Diffusion Equation (when $\alpha = 1$, $\beta = 1$, c and d are constants)

Case2 Part a: Fractional Diffusion Equation (when $0 < \alpha < 1$, $\beta = 1$, $d = 0$, c is constant)

Case2 Part b: Fractional Convection-Diffusion Equation (when $0 < \alpha < 1$, $\beta = 1$, d and c are constants).

In chapter two, we will discuss the analytic solution of FPE in one dimension for the previous cases using method of separation of variables. Furthermore, the existence and uniqueness will be shown too, especially, we will discuss the analytic solution in sections 2.2, 2.4 in details, which was not discussed in details in the previous books and periodicals.

In chapter three, we will present the numerical solution of FPE in one dimension for the previous cases, using explicit finite difference method. Moreover, we will investigate the stability of the numerical solution for the FPE. In particular, we will investigate the stability in section 3.3, which was not discussed in the previous books and periodicals to the approach used in the proof.

In the last chapter, we will discuss the solution of FPE in one dimension using the Langevin picture implemented Euler-Maruyama method. We study the appearance of transient fractional behavior due to the existence of confinement on a particle performing normal diffusion. Through this thesis, we have implemented our codes in Matlab environment.

CHAPTER ONE

PRELIMINARIES

In this chapter, we introduce some definitions and theorems that we will use throughout the thesis.

Definition. 1 [35]: Let $\alpha \in R_+$. The Riemann-Liouville definition integrals operator $I_{a+}^\alpha f$ and $I_{b-}^\alpha f$ are defined on the usual Lebesgue space $L_1(a, b)$ by

$$I_{a+}^\alpha f(x) = \frac{d^{-\alpha} f(x)}{dx^{-\alpha}} = \frac{1}{\Gamma(\alpha)} \int_a^x (x-t)^{\alpha-1} f(t) dt,$$

$$x > a, \operatorname{Re}(\alpha) > 0$$

$$I_{b-}^\alpha f(x) = \frac{d^{-\alpha} f(x)}{dx^{-\alpha}} = \frac{1}{\Gamma(\alpha)} \int_x^b (t-x)^{\alpha-1} f(t) dt, \quad x < b, \operatorname{Re}(\alpha) > 0$$

Definition. 2 [35]: The Riemann-Liouville fractional derivatives

$$D_{a+}^\alpha f \quad \text{and} \quad D_{b-}^\alpha f \quad \text{of order } \alpha \in C, \operatorname{Re}(\alpha) > 0, \quad n = [\alpha] + 1.$$

on the usual Lebesgue space $L_1(a, b)$ are defined by

$$D_{a+}^\alpha f(x) = \frac{d^\alpha f(x)}{dx^\alpha} = \frac{d^n}{dx^n} I^{n-\alpha} f(x) = \frac{1}{\Gamma(n-\alpha)} \frac{d^n}{dx^n} \int_a^x (x-t)^{n-\alpha-1} f(t) dt$$

$$D_{b-}^\alpha f(x) = \frac{d^\alpha f(x)}{dx^\alpha} = (-1)^n \frac{d^n}{dx^n} I^{n-\alpha} f(x)$$

$$= \frac{1}{\Gamma(n-\alpha)} \frac{d^n}{dx^n} \int_x^b (t-x)^{n-\alpha-1} f(t) dt$$

Definition. 3([35],[38]): The Caputo ${}^C D_{a+}^\alpha f$ and ${}^C D_{b-}^\alpha f$ of order $\alpha \in \mathbb{C}$, $\text{Re}(\alpha > 0)$.

on $[a, b]$ are defined by :

$$\begin{aligned} {}^C D_{a+}^\alpha f(x) &= \frac{d^\alpha f(x)}{dx^\alpha} = I^{n-\alpha} f^n(x) \\ &= \frac{1}{\Gamma(n-\alpha)} \int_a^x (x-t)^{n-\alpha-1} f^n(t) dt \\ {}^C D_{b-}^\alpha f(x) &= \frac{d^\alpha f(x)}{dx^\alpha} = I^{n-\alpha} f^n(x) \\ &= \frac{1}{\Gamma(n-\alpha)} \int_x^b (x-t)^{n-\alpha-1} f^n(t) dt \end{aligned}$$

Definition.4 [52]: The gamma function :

$$\Gamma(z) = \int_0^\infty t^{z-1} e^{-t} dt$$

Definition. 5 [24]: A one-parameter function of the Mittag-Leffler function is defined by the series expansion

$$E_\alpha(z) = (x+a)^n = \sum_{k=0}^n \frac{z^k}{\Gamma(\alpha k+1)} \quad z \in \mathbb{C}, \text{Re}(\alpha) > 0$$

Definition.6([35], [24]): A two-parameter function of the Mittag-Leffler function is defined by the series expansion :

$$E_{\alpha,\beta}(z) = \sum_{k=0}^n \frac{z^k}{\Gamma(\alpha k+\beta)} \quad z \in \mathbb{C}, \text{Re}(\alpha, \beta) > 0$$

Example: $E_{1,2}(z) = \frac{e^z - 1}{z}$

$$E_{2,2}(z) = \frac{\sinh(\sqrt{z})}{\sqrt{z}}$$

Theorem .7 [48]: Derivative of Mittag- Leffler

a. $\frac{d^n}{dt^n} [t^{\beta-1} E_{n,\beta}(\lambda t^n)] = t^{\beta-n-1} E_{n,\beta-n}(\lambda t^n)$

b. $E_{\alpha,\beta}^{(m)}(\lambda t^\alpha) = \sum_{m=1}^{\infty} \frac{\Gamma(\alpha k + 1)}{\Gamma(\alpha k - m + 1)} \frac{\lambda^k t^{\alpha k - m}}{\Gamma(\alpha k + \alpha m + \beta)}$

Theorem .8 [48]: Laplace Transform for the Mittag- Leffler

a. $L[E_{\alpha,\beta}(-at^\alpha)] = L\left[\sum_{m=0}^{\infty} \frac{(-a)^\alpha t^{m\alpha}}{\Gamma(\alpha m + \beta)}\right] = \frac{s^\alpha}{s(s^\alpha + a)}$,

b. $L[t^{\beta-1} E_{\alpha,\beta}(-at^\alpha)] = \frac{s^{\alpha-\beta}}{(s^\alpha + a)}$

c. $L[t^{\alpha m + \beta - 1} E_{\alpha,\beta}^{(m)}(-at^\alpha)] = \frac{m! s^{\alpha-\beta}}{(s^\alpha + a)^{m+1}}$

Definition.9 ([32] [39]): The statistical time average of a time series $x(t)$ is

defined by

$$\overline{(\delta^2(\Delta, t))} = \frac{1}{t-\Delta} \int_0^{t-\Delta} (x((t + \Delta) - \tau) - x(\tau))^2 d\tau$$

Definition.10 ([32; 39]): Ensemble average (EAMSD) at time t of many

trajectories $\{x(t')\}$ is defined as follows

$$\langle x^2(t) \rangle = \int_{-\infty}^{\infty} x^2 p(x) dx \quad \text{Where, } P(x) \text{ is the probability density distribution}$$

Definition.11 ([32], [46], [39]): Ergodic process, is a process in which statistical ensemble averages and long-time averages are equivalent in the limit of long measurement time (t_{max}) :

$$\overline{(\delta^2(\Delta, t_{max}))} = \langle x^2(\Delta, t_{max}) \rangle .$$

Definition .12 [4]: Gaussian distribution

$$f(x) = \frac{1}{\sigma\sqrt{2\pi}} e^{-\frac{(x-\mu)^2}{2\sigma^2}} , x \in R$$

Definition .13([35], [29]): The Laplace transform of continuous (or an almost piecewise continuous) function $f(t)$ in $[0, \infty)$ is defined as:

$$L\{f(t)\} = \int_0^{\infty} e^{-st} f(t) dt$$

Definition .14 [35] The Laplace transform of the Caputo fractional derivative is defined by:

$$L\{D^\alpha f(t)\} = s^\alpha F(s) - \sum_{k=0}^{n-1} s^{\alpha-k-1} f^{(k)}(0),$$

where $n - 1 \leq \alpha < n$.

Theorem .16 ([46]) : Weierstrass M-test.

Suppose that (f_n) is a sequence of real- or complex-valued functions defined on a set B , and that there is a sequence of non-negative numbers (C_n) satisfying the conditions:

$\sum |f_n(x)| \leq C_n$ for all $n \geq 1$, and all $x \in B$ and

$\sum_{n=1}^{\infty} C_n$ converges

Then the series, $\sum_{n=1}^{\infty} f_n(x)$ converges absolutely and uniformly on B .

Theorem .17 ([48], [56]): Abel's test in real analysis

Suppose the following statements are true,

1. $\sum a_n$ is a convergent series.
2. $\{f_n\}$ is a monotone sequence.
3. $\{f_n\}$ is bounded.

Then $\sum a_n f_n$ is also convergent.

Definition .18 ([35], [29]) :Fourier Transform

a: Fourier Transform:

$$\hat{u}(k, t) = \int_{-\infty}^{\infty} u(x, t) e^{-ikx} dx$$

b: Inverse Fourier Transform:

$$u(x, t) = \frac{1}{2\pi} \int_{-\infty}^{\infty} \hat{u}(k, t) e^{ikx} dk$$

Theorem .19 [42] : Coercivity Inequality

$$0 \leq \cos\left(\frac{\alpha\pi}{2}\right) \int_0^{t_n} \left| {}^C D_{a+}^{1-\frac{\alpha}{2}} v(t) \right|^2 dt \leq \int_0^{t_n} {}^C D_{a+}^{1-\alpha} v(t) \dot{v}(t) dt .$$

CHAPTER TWO

Analytic Solution of Fokker-Planck Equation.

In this chapter, we solve the Fokker-Planck equation with some cases by using separation of variables Method. In addition, we show the existence and uniqueness of the solution.

The method of separation is used to solve initial boundary-value problems involving linear partial differential equations. Usually, the dependent variable $u(x, y)$ is expressed in the separable form $u(x, y) = X(x) Y(y)$, where X and Y are functions of x and y respectively.

2.1 Analytic Solution of Diffusion Equation.

Consider the Fokker-Planck equation (1.1.1) with $\alpha = 1, \beta = 1, d = 0$, C is constant as in references [26] and [3]. We show the existence and uniqueness for this case. In this case, the Fokker-Planck equation admits the following form

$$u_t = c u_{xx}, \quad 0 < x < L, \quad t > 0 \quad (2.1.1)$$

Which is called diffusion equation.

In this section, we solve diffusion equation (2.1.1) analytically. The existence and uniqueness of the solution of equation (2.1.1) will be shown. In the next

two chapters we will solve (2.1.1) numerically by using explicit finite difference method and will discuss the fundamental solution of (2.1.1)

in one dimension using the Langevin picture using Monte Carlo simulation with the implementation of Euler-Maruyama method.

Suppose that the length of the bar L with the dirichlet boundary condition :

$$u(0, t) = 0, \quad u(L, t) = 0 \quad t \geq 0$$

and initial condition:

$$u(x, 0) = f(x), \quad \text{where } f(x) \text{ is continuous, } 0 \leq x \leq L$$

Where c is a positive constant. In fact c , sometimes called the thermal diffusivity of the bar, is given by $c = \frac{\kappa}{s\rho}$

κ = thermal conductivity of the material of the bar

s = specific heat capacity of the material of the bar

ρ = density of the material of the bar.

To solve equation (2.1.1), we use separation of variables method.

So, the solution is assumed to be of the form :

$$u(x, t) = X(x)T(t) \neq 0$$

$$u_t(x, t) = X(x) T'(t) \tag{2.1.2}$$

$$u_{xx}(x, t) = X''(x)T(t) \tag{2.1.3}$$

We substitute (2.1.2) and (2.1.3) into (2.1.1), then we have

$$X(x)T'(t) = c X''(x)T(t)$$

Thus, we have

$$\frac{X''(x)}{X(x)} = \frac{T'(t)}{c T(t)} = \lambda$$

Thus,

$$X(0) = 0, \quad X(L) = 0,$$

We have three cases:

Case(1): If $\lambda = 0$, then $X''(x) = 0$

$$X(x) = c_1x + c_2$$

By using the boundary conditions, we have

$$X(x) = 0 \rightarrow u(x, t) = 0$$

Case(2): If $\lambda > 0$, then we let $\lambda = D^2 > 0$

$$X''(x) - D^2X(x) = 0 \quad (2.1.4)$$

The solution of (2.1.4) is

$$X(x) = c_1e^{Dx} + c_2e^{-Dx}$$

By using the boundary conditions, we have

$$c_1 + c_2 = 0$$

$$c_1 e^{DL} + c_2 e^{-DL} = 0$$

From the previous two equations, we obtain

$$X(x) = 0$$

So, $u(x, t) = 0$

Case(3): If $\lambda < 0$, then we let $\lambda = -D^2 < 0$

$$\frac{X''(x)}{X(x)} = \frac{T'(t)}{c T(t)} = -D^2$$

$$\frac{X''(x)}{X(x)} = -D^2 \quad \text{and} \quad \frac{T'(t)}{c T(t)} = -D^2$$

Where D is a positive constant. Hence, X and T must satisfy

$$\dot{X}(x) + D^2 X(x) = 0 \tag{2.1.5}$$

$$T'(t) + c D^2 T(t) = 0 \tag{2.1.6}$$

Hence, we must solve the eigenvalue problem

$$X''(x) + D^2 X(x) = 0$$

$$X(0) = 0, X(L) = 0.$$

The solution of equation (2.1.5) is

$$X(x) = A \cos Dx + B \sin Dx.$$

Since $X(0) = 0$, $A = 0$. To satisfy the second condition, we have

$$X(L) = B \sin DL = 0.$$

Since $B = 0$ yields a trivial solution, we must have $B \neq 0$ and hence

$$\sin DL = 0.$$

Thus,

$$D = \frac{n\pi}{L}$$

for $n = 1, 2, 3, \dots$

Substituting these eigenvalues, we have

$$X_n(x) = B_n \sin\left(\frac{n\pi}{L}x\right)$$

Next, we consider equation (2.1.6), namely

$$T'(t) + cD^2 T(t) = 0,$$

the solution of which is:

$$T(t) = Ce^{-D^2 ct}.$$

Substituting $D = (n\pi/L)$, we have

$$T_n(t) = C_n e^{-\left(\frac{n\pi}{L}\right)^2 ct}$$

Hence, the nontrivial solution of the heat equation which satisfies the two

boundary conditions is $u_n(x, t) = a_n e^{-\left(\frac{n\pi}{L}\right)^2 ct} \sin\left(\frac{n\pi}{L}x\right)$

where $a_n = B_n C_n$ is an arbitrary constant.

By the principle of superposition, we obtain a formal series solution as

$$u(x, t) = \sum_{n=0}^{\infty} X_n(x) T_n(t)$$

$$u(x, t) = \sum_{n=0}^{\infty} a_n e^{-\left(\frac{n\pi}{L}\right)^2 ct} \sin\left(\frac{n\pi}{L}x\right)$$

which satisfies the initial condition if

$$u(x, 0) = f(x) = \sum_{n=0}^{\infty} a_n \sin\left(\frac{n\pi}{L}x\right)$$

Where

$$a_n = \frac{1}{2L} \int_0^L f(x) \sin\left(\frac{n\pi}{L}x\right) dx$$

Hence,

$$u(x, t) = \sum_{n=0}^{\infty} \left(\frac{1}{2L} \int_0^L f(x) \sin\left(\frac{n\pi}{L}x\right) dx \right) e^{-\left(\frac{n\pi}{L}\right)^2 ct} \sin\left(\frac{n\pi}{L}x\right) \quad (2.1.7)$$

Remark: In the following figures, we consider the sum is finite.

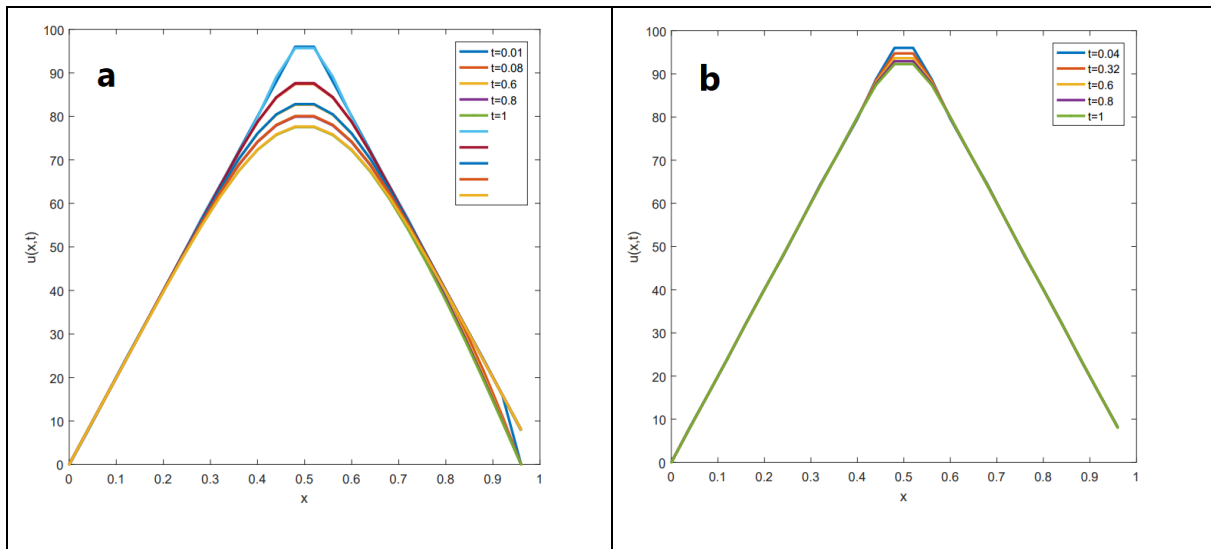


Figure (2.1.1): Analytic solution of diffusion equation with time step $k=0.04$ and $c= 0.01 \text{ cm}^2/\text{s}$ in figure (a) and $0.001 \text{ cm}^2 / \text{s}$ in figure (b), and Dirichlet boundary condition.

The next figure shows the analytic solution of diffusion equation with Neumann boundary condition ($u_x(0, t) = u_x(L, t) = 0$).

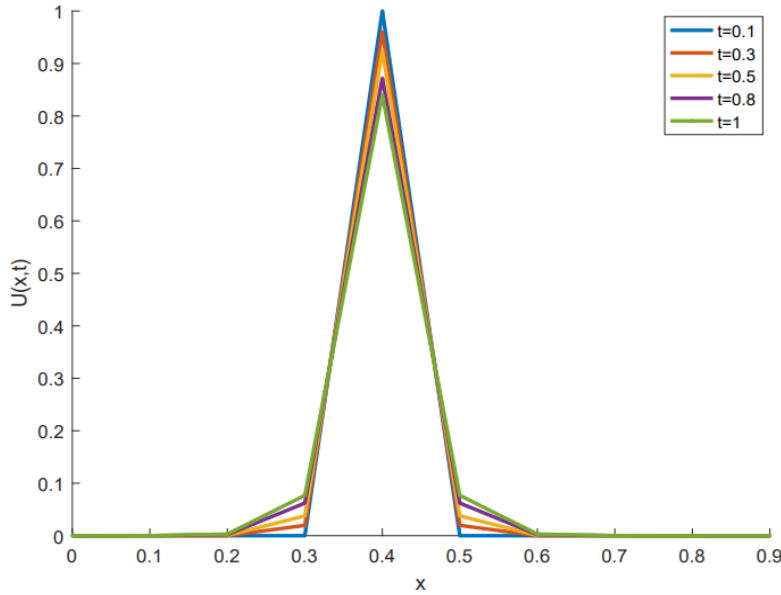


Figure (2.1.2): Analytic solution of diffusion equation with Neumann boundary condition.

To study the existence of the solution of equation (2.1.1), we state the following theorem.

Theorem (2.1.2) [[35],7] : If $f(x)$ is continuous in $[0, L]$ and $f(0) = f(L) = 0$, and $\dot{f}(x)$ is piecewise continuous in $(0, L)$. Then there is a solution for equation (2.1.1)

Proof: Since $f(x)$ is bounded, we have

$$|a_n| = \left| \frac{2}{L} \int_0^L f(x) \sin\left(\frac{n\pi x}{L}\right) dx \right| \leq \frac{2}{L} \int_0^L f(x) dx \leq m.$$

where m is a positive constant. Thus, for any finite $t_0 > 0$,

$$\left| a_n e^{-(n\pi/L)^2 ct} \sin\left(\frac{n\pi x}{L}\right) \right| \leq m e^{-(n\pi/L)^2 ct_0} \text{ when } t \geq t_0.$$

According to the ratio test, the series of terms $\exp[-(n\pi/L)^2 t_0]$ converges.

Hence, by the Weierstrass M-test as stated in the previous chapter, the series

$$\sum_{n=1}^{\infty} a_n e^{-(n\pi/L)^2 ct} \sin\left(\frac{n\pi x}{L}\right) \quad (2.1.8)$$

converges uniformly with respect to x and t whenever $t \geq t_0$ and $0 \leq x \leq L$.

Differentiating the series (2.1.8) with respect to t , we obtain

$$u_t = - \sum_{n=1}^{\infty} a_n \left(\frac{n\pi}{L}\right)^2 c e^{-(\frac{n\pi}{L})^2 ct} \sin\left(\frac{n\pi x}{L}\right) \quad (2.1.9)$$

We note that

$$\left| - a_n \left(\frac{n\pi}{L}\right)^2 c e^{-(n\pi/L)^2 ct} \sin\left(\frac{n\pi x}{L}\right) \right| \leq m c \left(\frac{n\pi}{L}\right)^2 e^{-(\frac{n\pi}{L})^2 ct_0}.$$

hence $t \geq t_0$ and the series of terms $m c (n\pi x/L)^2 \exp\left[-\left(\frac{n\pi}{L}\right)^2 ct_0\right]$

Converges by the ratio test. Hence, equation (2.1.9) is uniformly convergent in

The region $0 \leq x \leq L$ and $t \geq t_0$. In a similar manner, the series (2.1.8) can

be differentiated twice with respect to x , and as a result

$$u_{xx} = - \sum_{n=1}^{\infty} a_n \left(\frac{n\pi x}{L}\right)^2 e^{-(\frac{n\pi}{L})^2 ct} \sin\left(\frac{n\pi x}{L}\right) \quad (2.1.10)$$

From equations (2.1.9) and (2.1.10), we obtain

$$u_t = c u_{xx}$$

Hence, equation (2.1.8) is a solution of the one-dimensional diffusion equation in the region $0 \leq x \leq L$, $t > 0$.

Next, we show that the boundary conditions are satisfied. Here, we note that the series (2.1.8) representing the function $u(x, t)$ converges uniformly in the region $0 \leq x \leq L$, $t \geq 0$.

Since the function represented by a uniformly convergent series of continuous functions is continuous, $u(x, t)$ is continuous at $x = 0$ and $x = L$. As a consequence, when $x = 0$ and $x = L$ solution (2.1.7) satisfies

$$u(0, t) = 0, \quad u(L, t) = 0,$$

for all $t > 0$.

It remains to show that $u(x, t)$ satisfies the initial condition

$$u(x, 0) = f(x), \quad 0 \leq x \leq L$$

Under the assumptions stated in the first section, the series for $f(x)$ is given by

$$f(x) = \sum_{n=1}^{\infty} a_n \sin\left(\frac{n\pi x}{L}\right)$$

is uniformly and absolutely convergent. By Abel's test [56] of convergence the series formed by the product of the terms of a uniformly convergent series

$$\sum_{n=1}^{\infty} a_n \sin\left(\frac{n\pi x}{L}\right)$$

and a uniformly bounded and monotone sequence $\exp\left[-\left(\frac{n\pi}{L}\right)^2 ct_0\right]$

converges uniformly with respect to t . Hence,

$$u(x, t) = \sum_{n=1}^{\infty} a_n e^{-(n\pi/L)^2 ct} \sin\left(\frac{n\pi x}{L}\right)$$

converges uniformly for $0 \leq x \leq L$, $t \geq 0$. By the same reason as before,

$u(x, t)$ is continuous for $0 \leq x \leq L$, $t \geq 0$. Thus, the initial condition

$$u(x, 0) = f(x), \quad 0 \leq x \leq L$$

is satisfied.

The next theorem shows the uniqueness for equation (2.1.1).

Uniqueness Theorem (2.1.1) [44], [45]: Let $u(x, t)$ be a continuously differentiable function.

If $u(x, t)$ satisfies the differential equation (2.1.1),

$$u_t = c u_{xx}, \quad 0 < x < L, \quad t > 0$$

and initial condition

$$u(x, 0) = f(x), \quad 0 \leq x \leq L$$

with Dirichlet boundary conditions

$$u(0, t) = 0, \quad u(L, t) = 0, \quad t \geq 0$$

then, the solution is unique.

Proof. Suppose that there are two distinct solutions $u_1(x, t)$ and $u_2(x, t)$.

Let $v(x, t) = u_1(x, t) - u_2(x, t)$

Then

$$v_t = c v_{xx}, \quad 0 < x < L, \quad t > 0$$

$$v(0, t) = 0, \quad v(L, t) = 0, \quad t \geq 0$$

$$v(x, 0) = 0, \quad 0 \leq x \leq L. \quad (2.1.11)$$

Consider the function defined by the integral

$$I(t) = \frac{1}{2c} \int_0^L v^2 dx$$

Differentiating with respect to t , we have

$$I'(t) = \frac{1}{2c} \int_0^L v v_t dx = \int_0^L v v_{xx} dx,$$

by using (2.1.11) and integrating by parts, we have

$$\int_0^L v v_{xx} dx = [v v_x]_0^L - \int_0^L v_x^2 dx,$$

Since $v(0, t) = 0, v(L, t) = 0$

$$I'(t) = - \int_0^L v_x^2 dx \leq 0.$$

From the condition $v(x, 0) = 0$, we have $I(0) = 0$. This condition and

$I'(t) \leq 0$ implies that $I(t)$ is a nonincreasing function of t . Thus,

$$I(t) \leq 0 \quad (2.1.12)$$

But by definition of $I(t)$

$$I(t) \geq 0 \quad (2.1.13)$$

From (2.1.12) and (2.1.13)

$$I(t) = 0 \quad \text{for } t \geq 0$$

Since $v(x, t)$ is continuous, $I(t) = 0$ implies that

$$v(x, t) = 0.$$

In $0 \leq x \leq L$, $t \geq 0$. Hence, $u_1 = u_2$ and the solution is unique.

Example (2.1.1): Find the temperature distribution in a rod of length l . The faces are insulated, and the initial temperature distribution is given by

$$u(x, 0) = x(1 - x).$$

or, solve the following PDE

$$u_t = c u_{xx} \quad , \quad 0 < x < 1 \quad , \quad t > 0 \quad (2.1.1)$$

$$u(0, t) = 0 \quad , \quad t \geq 0$$

$$u(l, t) = 0 \quad , \quad t \geq 0$$

$$u(x, 0) = x(1 - x) \quad , \quad 0 < x < 1$$

$$a_n = \frac{1}{2L} \int_0^L x(1 - x) \sin\left(\frac{n\pi}{L} x\right) dx = \frac{8}{(2n - 1)^3 \pi^3}$$

$$u(x, t) = \sum_{n=1}^{\infty} \left(\frac{8}{(2n-1)^3 \pi^3} \right) e^{-\left(\frac{(2n-1)\pi}{L}\right)^2 ct} \sin\left(\frac{(2n-1)\pi}{L} x\right)$$

Example (2.1.2): Solve the following PDE

$$u_t = cu_{xx} \quad , \quad 0 < x < L \quad , \quad t > 0$$

$$u(0, t) = 0 \quad , \quad t \geq 0$$

$$u(L, t) = u_0 \quad , \quad t \geq 0$$

$$u(x, 0) = x(L - x) \quad , \quad 0 < x < L$$

Let

$$u(x, t) = v(x, t) + \frac{u_0}{L} x$$

Substitution of $u(x, t)$ in equations (2.1.1) yields

$$v_t = cv_{xx} \quad , \quad 0 < x < L \quad , \quad t > 0 \tag{2.1.14}$$

$$v(0, t) = 0 \quad , \quad t \geq 0$$

$$v(L, t) = 0 \quad , \quad t \geq 0$$

$$v(x, 0) = x(L - x) - \frac{u_0}{L} x \quad , \quad 0 < x < L$$

$$v(x, t) = \sum_{n=0}^{\infty} \left(\frac{1}{2L} \int_0^L (f(x) - \frac{u_0}{L}x) \sin\left(\frac{n\pi}{L}x\right) dx \right) e^{-\left(\frac{n\pi}{L}\right)^2 ct} \sin\left(\frac{n\pi}{L}x\right) + \frac{u_0}{L}x$$

Remark: The solution of equation (2.1.1) $u_t = c u_{xx}$; $0 < x < L$, $t > 0$

with Neumann conditions

$$u_x(0, t) = 0, \quad u_x(L, t) = 0 \quad t \geq 0$$

and initial condition

$$u(x, 0) = f(x) \quad , \quad 0 \leq x \leq L$$

is

$$u(x, t) = \sum_{n=1}^{\infty} a_n e^{-(n\pi/L)^2 ct} \cos\left(\frac{n\pi x}{L}\right)$$

Where $a_n = \frac{1}{2L} \int_0^L f(x) \cos\left(\frac{n\pi}{L}x\right) dx$

2.2 Analytic Solution of Convection-Diffusion Equation.

In this section, we study the solution of the Fokker-Planck equation (1.1.1)

when $\alpha = 1$, $\beta = 1$, d and c are constants and we show the existence and

uniqueness for this case. Then the Fokker-Planck equation becomes

$$u_t = -d u_x + c u_{xx} \tag{2.2.1}$$

With $u(0, t) = A$, $u(L, t) = B$

$$u(x, 0) = f(x)$$

$$\text{Let } u(x, t) = v(x, t) + G(x)$$

We differentiate $u(x, t)$ with respect to t and to x , then we have

$$u_t = v_t \tag{2.2.2}$$

$$u_x = v_x + G'(x) \tag{2.2.3}$$

$$u_{xx} = v_{xx} + G''(x) \tag{2.2.4}$$

$$u(x, 0) = v(x, 0) + G(0)$$

$$v(x, 0) = f(x) - G(0)$$

Substituting equations (2.2.2) , (2.2.3) and (2.2.4) in equation (2.2.1), the we get

$$v_t = -d(v_x + G'(x)) + c(v_{xx} + G''(x))$$

$$v_t = -dv_x + cv_{xx} + (-dG'(x) + cG''(x)) \tag{2.2.5}$$

$$u(0, t) = v(0, t) + G(0) = A$$

$$u(l, t) = v(L, t) + G(L) = B$$

$$\text{If } -dG'(x) + cG''(x) = 0$$

With $G(0) = A$, $G(L) = B$, then

$$-dr + cr^2 = 0 , \text{ or}$$

$$r = 0, r = \frac{d}{c}$$

So, $G(x) = c_1 + c_2 e^{\frac{dx}{c}}$

Then, equation (2.2.5) admits the following form

$$v_t = -d v_x + c v_{xx} \tag{2.2.6}$$

If $v(0, t) = 0, v(L, t) = 0,$ and $v(x, 0) = f(x) - G(x)$

To solve equation (2.2.6) , let $v(x, t) = X(x)T(t)$

Then, we have

$$c \frac{X''(x)}{X(x)} - d \frac{X'(x)}{X(x)} = \frac{T'(t)}{T(t)} = \lambda < 0$$

$$c \frac{X''(x)}{X(x)} - d \frac{X'(x)}{X(x)} = \lambda \quad \text{and} \quad \frac{T'(t)}{T(t)} = \lambda$$

Hence, X and T must satisfy

$$c X''(x) - dX'(x) - \lambda X(x) = 0 \tag{2.2.7}$$

$$T'(t) - \lambda T(t) = 0 \tag{2.2.8}$$

Hence, we must solve the eigenvalue problem

$$c X''(x) - dX'(x) - \lambda X = 0,$$

$$X(0) = 0, X(L) = 0.$$

The characteristic equation for equation (2.2.7) is

$$cr^2 - dr - \lambda = 0$$

if $d^2 + 4\lambda c \geq 0,$ we get the trivial solution $u(x,t)=0.$

Now, if $d^2 + 4\lambda c < 0,$ then, the solution of the characteristic equation is

$$r = \frac{d \mp \sqrt{d^2 + 4\lambda c}}{2c} = \frac{d}{2c} \mp \frac{\sqrt{-d^2 - 4\lambda c}}{2c} i$$

Thus,

$$X(x) = e^{\frac{dx}{2c}} \left(A \cos \left(\frac{\sqrt{-d^2 - 4\lambda c}}{2c} x \right) + B \sin \left(\frac{\sqrt{-d^2 - 4\lambda c}}{2c} x \right) \right)$$

Since $X(0) = 0$, then $A = 0$. To satisfy the second condition, $X(L) = 0$, we have

$$X(L) = B \sin \left(\frac{\sqrt{-d^2 - 4\lambda c}}{2c} L \right) = 0.$$

Since $B = 0$ yields a trivial solution, we must have $B \neq 0$ and hence

$$\sin \left(\frac{\sqrt{-d^2 - 4\lambda c}}{2c} L \right) = 0.$$

Thus,

$$\left(\frac{\sqrt{-d^2 - 4\lambda c}}{2c} \right) L = \frac{n\pi}{L}$$

$$\text{for } n = 1, 2, 3, \dots$$

Substituting these eigenvalues, we have

$$X_n(x) = B_n e^{\frac{dx}{2c}} \sin \left(\frac{n\pi}{L} x \right)$$

To solve equation (2.2.8), we follow the same steps that we used in section

(1.1) to obtain $T_n(t) = D_n e^{-\lambda_n t}$

$$\text{Where } \lambda_n = \frac{d^2}{4c} + \frac{n^2 \pi^2 c}{L}$$

Hence, the nontrivial solution of the convection equation which satisfies the

Dirichlet boundary conditions is $v(x, t) = a_n e^{\frac{dx}{2c}} e^{-\lambda_n t} \sin\left(\frac{n\pi}{L} x\right)$

where $a_n = B_n D_n$ is an arbitrary constant.

By the principle of superposition, we obtain a formal series solution as

So,

$$v(x, t) = \sum_{n=0}^{\infty} X_n(x) T_n(t)$$

$$v(x, t) = \sum_{n=0}^{\infty} a_n e^{\frac{dx}{2c}} e^{-\lambda_n t} \sin\left(\frac{n\pi}{L} x\right)$$

which satisfies the initial condition if

$$v(x, 0) = f(x) - G(x) = \sum_{n=0}^{\infty} a_n e^{\frac{dx}{2c}} \sin\left(\frac{n\pi}{L} x\right)$$

Where

$$a_n = \frac{1}{2L} \int_0^L (f(x) - G(x)) \sin\left(\frac{n\pi}{L} x\right) e^{\frac{dx}{2c}} dx$$

Hence ,

$$u(x, t) = \sum_{n=0}^{\infty} (f(x) - G(x)) e^{\frac{dx}{2c}} e^{-\lambda_n t} \sin\left(\frac{n\pi}{L} x\right).$$

The following theorem shows the uniqueness of the solution for convection-diffusion equation.

Uniqueness Theorem (2.2.1): Suppose that $u(x, t)$ is continuously differentiable function. If $u(x, t)$ satisfies the differential equation

$$u_t = -d u_x + cu_{xx}, \quad 0 < x < L, \quad t > 0$$

And initial condition:

$$u(x, 0) = f(x), \quad 0 \leq x \leq L$$

With the boundary condition:

$$u(0, t) = A, \quad u(L, t) = B \quad t \geq 0.$$

Then, the solution is unique.

Proof. We use the same manner that we used in theorem (2.1.1) to prove our theorem (2.2.1).

Next, we prove the existence of the solution of equation (2.2.1)

Theorem (2.2.2) : If $f(x)$ is continuous in $[0, L]$ and $f(0) = f(L) = 0$. and $f'(x)$ is piecewise continuous in $(0, L)$. Then there is a solution for equation (2.2.1)

Proof: We use the same manner that we used in the proof theorem (2.1.1)

To obtain

$$|a_n| = \left| \frac{2}{L} \int_0^L f(x) \sin\left(\frac{n\pi x}{L}\right) dx \right| \leq \frac{2}{L} \int_0^L f(x) dx \leq m.$$

where m is a positive constant. Thus, for any finite $t_0 > 0$,

$$\left| a_n e^{-\lambda t + \frac{dx}{2c}} \sin\left(\frac{n\pi x}{L}\right) \right| \leq m e^{-\lambda t_0 + \frac{dl}{2c}} \quad \text{when } t \geq t_0.$$

$$u_t = - \sum_{n=1}^{\infty} a_n \lambda e^{-\lambda t + \frac{dx}{2c}} \sin\left(\frac{n\pi x}{L}\right) \quad (2.2.9)$$

We note that

$$\left| - a_n \lambda e^{-\lambda t + \frac{dx}{2c}} \sin\left(\frac{n\pi x}{L}\right) \right| \leq m a_n \lambda e^{-\lambda t_0 + \frac{dl}{2c}}$$

$$u_{xx} = - \sum_{n=1}^{\infty} a_n \left(\frac{n\pi x}{L}\right)^2 e^{-\lambda t + \frac{dx}{2c}} \sin\left(\frac{n\pi x}{L}\right). \quad (2.2.10)$$

From equations (2.2.9) and (2.2.10), we have

$$u_t = -du_x + c u_{xx}$$

Hence, equation (2.2.1) is a solution of the one-dimensional convection diffusion equation in the region $0 \leq x \leq L$, $t \geq 0$.

And equation (2.2.1) satisfies

$$u(0, t) = A, \quad u(L, t) = B,$$

For all, $t > 0$.

Moreover, $u(x, t)$ satisfies the initial condition

$$u(x, 0) = f(x), \quad 0 \leq x \leq L$$

Example(2.2.1): Solve the following equation

$$u_t = -d u_x + c u_{xx}, \quad 0 < x < L$$

With $u(0, t) = 0$, $u(L, t) = 100$

$$u(x, 0) = 100x/L$$

Let $u(x, t) = v(x, t) + G(x)$

$$v(x, t) = \sum_{n=0}^{\infty} a_n e^{\frac{dx}{2c}} e^{-\lambda t} \sin\left(\frac{n\pi}{L}x\right)$$

$$a_n = \frac{1}{2L} \int_0^L (f(x) - U(x)) \sin\left(\frac{n\pi}{L}x\right) e^{\frac{-dx}{2c}} dx$$

$$U(x) = \frac{100}{e^p - 1} \left(1 - e^{\frac{px}{L}}\right), \text{ where } p = \frac{dx}{L}$$

$$I_1 = \frac{1}{2L} \int_0^L \frac{100x}{L} \sin\left(\frac{n\pi}{L}x\right) e^{\frac{-px}{2L}} dx$$

$$= 200 n\pi \left(\frac{(-1)^{n+1} e^{-\frac{p}{2}}}{\frac{p^2}{4} + n^2\pi^2} + \frac{(-1)^{n+1} e^{-\frac{p}{2}}}{\left(\frac{p^2}{4} + n^2\pi^2\right)^2} + \frac{p}{\left(\frac{p^2}{4} + n^2\pi^2\right)^2} \right)$$

$$I_2 = \frac{100}{2L} \int_0^L \sin\left(\frac{n\pi}{L}x\right) e^{\frac{px}{2L}} dx$$

$$= 200 n\pi \left(\frac{(-1)^{n+1} e^{-\frac{p}{2}}}{\frac{p^2}{4} + n^2\pi^2} + \frac{(-1)^{n+1} e^{-\frac{p}{2}}}{\left(\frac{p^2}{4} + n^2\pi^2\right)^2} + \frac{p}{\left(\frac{p^2}{4} + n^2\pi^2\right)^2} \right)$$

$$I_2 = \frac{100}{2L} \int_0^L \sin\left(\frac{n\pi}{L}x\right) e^{\frac{px}{2L}} dx$$

$$= 200 n\pi \left(\frac{1}{\frac{p^2}{4} + n^2\pi^2} + \frac{(-1)^{n+1}e^{\frac{p}{2}}}{\frac{p^2}{4} + n^2\pi^2} \right)$$

$$I_3 = \frac{100}{2L} \int_0^1 \sin\left(\frac{n\pi}{L}x\right) e^{\frac{-px}{2L}} dx$$

$$= 200 n\pi \left(\frac{1}{\frac{p^2}{4} + n^2\pi^2} + \frac{(-1)^{n+1}e^{\frac{-p}{2}}}{\frac{p^2}{4} + n^2\pi^2} \right)$$

$$\text{So, } u(x, t) = 100 \left(\frac{e^{\frac{px}{L}} - 1}{e^p - 1} + \frac{4\pi e^{\frac{px}{2L}} \sinh\left(\frac{p}{2}\right)}{e^p - 1} + \sum_{n=1}^{\infty} A_n + 4\pi e^{\frac{px}{2L}} \sum_{n=1}^{\infty} B_n \right)$$

$$A_n = (-1)^n n \beta_n^{-1} \sin\left(\frac{n\pi}{L}x\right) e^{-\lambda_n t}$$

$$B_n = \left[(-1)^{n+1} n \beta_n^{-1} (n \beta_n^{-1}) e^{-\frac{p}{2}} + \frac{np}{\beta_n^2} \right] \sin\left(\frac{n\pi}{L}x\right) e^{-\lambda_n t}$$

$$\beta_n = \frac{p^2}{4} + n^2\pi^2$$

$$\lambda_n = \frac{d^2}{4c} + \frac{n^2\pi^2 c}{L}$$

2.3 Analytic Solution of Fractional Diffusion Equation.

This section is devoted to study the existence and uniqueness of the solution of the Fokker-Planck equation (1.1.1) when $0 < \alpha < 1$, $\beta = 1$,

$d = 0$ and C is constant [40]. With the chosen parameters, equation

(1.1.1) admits the following form

$${}_t^c D_{0+}^{1-\alpha} u(x, t) = \frac{\partial u^{1-\alpha}}{\partial t^{1-\alpha}} = c \frac{\partial^2 u}{\partial x^2}, \quad (2.3.1)$$

with initial condition $u(x, 0) = f(x)$

To solve (2.3.1), we let $U(x, t) = X(x)T(t)$

If $\lambda < 0$, then we have

$$\frac{X''(x)}{X(x)} = \frac{\partial T^\alpha}{c T \partial t^\alpha} = \lambda$$

$$X''(x) - \lambda X(x) = 0 \quad \text{and} \quad \frac{\partial u^\alpha}{c T(t)} = \lambda$$

Hence, X and T must satisfy

$$X''(x) - \lambda X(x) = 0 \quad (2.3.2)$$

$$\frac{\partial T^\alpha}{\partial t^\alpha} - \lambda c T(t) = 0 \quad (2.3.3)$$

Hence, we must solve the eigenvalue problem

$$X''(x) - \lambda X = 0,$$

$$X(0) = 0, X(L) = 0.$$

To solve equation (2.3.2), we follow the same steps that we used in section (1.1)

and we get

$$X_n(x) = B_n \sin\left(\frac{n\pi}{L}x\right)$$

Next, we want to solve equation (2.3.3), namely,

$$\frac{\partial T^\alpha}{\partial t^\alpha} - \lambda c T(t) = 0$$

$$\text{Where } \frac{\partial T^\alpha}{\partial t^\alpha} = \int_0^t \frac{(t-s)^{\alpha-1}}{\Gamma(\alpha)} T'(s) ds = \frac{(t)^{\alpha-1}}{\Gamma(\alpha)} * T'(t)$$

$$\text{Such that, } (f * g)(t) = \int_0^t f(t-s)g(s)ds$$

Taking Laplace for both sides for eq. (2.3.3) with respect to t

$$\text{and using } L(T'(t)) = sL(T(t)) - T(0)$$

$$\text{with } L(f(t) * g(t)) = L(f(t)) L(g(t))$$

Then we have,

$$L\left(\frac{t^{\alpha-1}}{\Gamma(\alpha)} * T'(t)\right) = \lambda c \bar{T}(s), \text{ where } \bar{T}(s) = L(f(t)).$$

Or

$$\frac{1}{s^\alpha} (s\bar{T}(s) - T(0)) = \lambda c \bar{T}(s)$$

$$\lambda c \bar{T}(s) - s^{-\alpha+1} \bar{T}(s) = -s^{-\alpha} T(0)$$

$$\bar{T}(s) = \frac{s^{-\alpha} T(0)}{s^{-\alpha+1} - \lambda c}$$

Taking Laplace inverse and using the following formula:

$$L\{t^{m\alpha+\beta-1} E_{\alpha,\beta}^{(m)}(-at^\alpha)\} = \frac{m! s^{\alpha-\beta}}{(s^\alpha + a)^{m+1}}$$

Then, we have:

$$T(t) = T(0) E_{1-\alpha,1}(-\lambda ct^{1-\alpha})$$

the solution of (2.3.1) is

$$T_n(t) = T(0) E_{1-\alpha,1}(-\lambda ct^{1-\alpha}) = T(0) E_{1-\alpha,1}\left(-\frac{n\pi}{L} ct^{1-\alpha}\right)$$

Hence,

$$u(x, t) = \sum_{n=0}^{\infty} X_n(x) T_n(t)$$

$$u(x, t) = \sum_{n=0}^{\infty} a_n E_{1-\alpha,1}\left(-\frac{n\pi}{L} ct^{1-\alpha}\right) \sin\left(\frac{n\pi}{L} x\right)$$

which satisfies the initial condition if

$$u(x, 0) = f(x) = \sum_{n=0}^{\infty} a_n \sin\left(\frac{n\pi}{L} x\right)$$

Where

$$a_n = \frac{1}{2L} \int_0^L f(x) \sin\left(\frac{n\pi}{L} x\right) dx$$

Hence ,

$$u(x, t) = \sum_{n=0}^{\infty} a_n E_{1-\alpha,1}\left(-\frac{n\pi}{L} ct^{1-\alpha}\right) \sin\left(\frac{n\pi}{L} x\right)$$

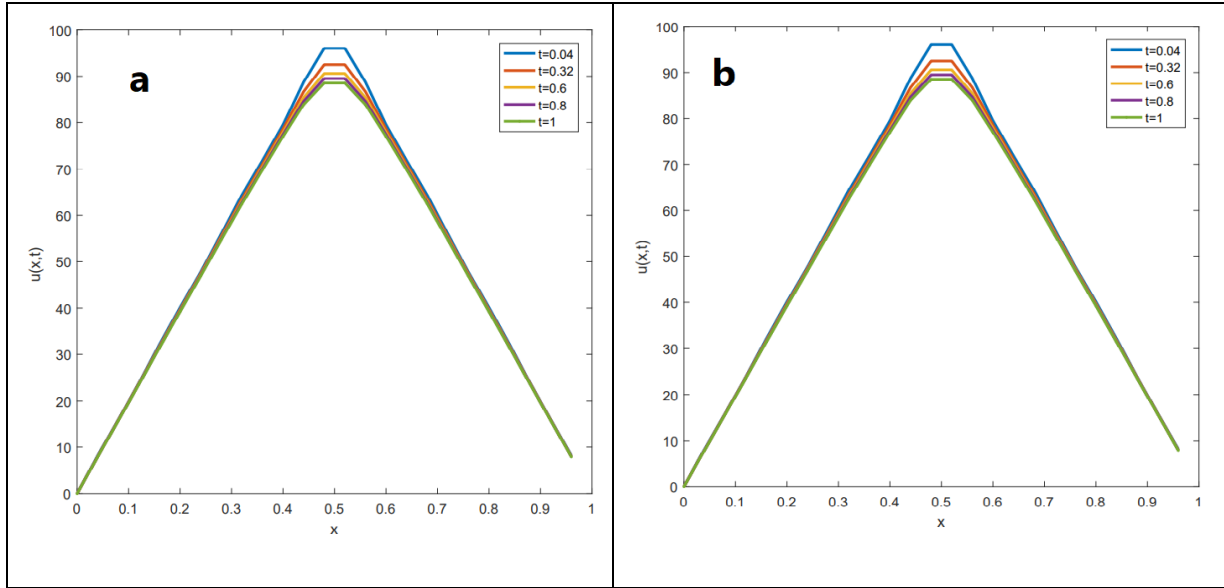


Figure (2.2.1) Analytic solution of fractional diffusion equation with time step $k=0.04$ and $c=0.001 \text{ cm}^2/\text{s}$ and $\alpha=0.3$ in part(a), $\alpha=0.5$ in part (b).

Uniqueness Theorem (2.2.1): Suppose that $u(x, t)$ is continuously differentiable function. If $u(x, t)$ satisfies the differential equation

$${}_t^C D_{0+}^{1-\alpha} u(x, t) = c u_{xx}, \quad 0 \leq x \leq L, \quad t \geq 0.$$

$$u(x, 0) = f(x)$$

$$u(0, t) = 0, \quad u(L, t) = 0,$$

Then, the solution is unique.

Proof: Let $u_1(x, t)$ and $u_2(x, t)$ be two distinct solutions.

and let $v = u_1 - u_2$, then we have

$${}_t^C D_{0+}^{1-\alpha} v(x, t) = c v_{xx} \tag{2.3.4}$$

$$, \quad 0 \leq x \leq L, \quad t \geq 0.$$

$$v(x, 0) = 0$$

$$v(0, t) = 0, \quad v(L, t) = 0,$$

Multiply equation (2.3.4) by v_t for both sides, then we have

$${}_t^c D_{0+}^{1-\alpha} v(x, t) v_t(x, t) = c v_{xx} v_t(x, t).$$

Taking the integral from 0 to L with respect to x , then we obtain

$$\int_0^L {}_t^c D_{0+}^{1-\alpha} v v_t(x, t) dx - \int_0^L c v_{xx} v_t(x, t) dx = 0 \quad (2.3.5)$$

Now,

$$\begin{aligned} & \int_0^L c v_{xx} v_t(x, t) dx = \\ & c v_x(L, t) v_t(L, t) - c v_x(0, t) v_t(0, t) - c \int_0^L v_{tx} v_x(x, t) dx = \\ & -c \int_0^L v_{tx} v_x(x, t) dx \end{aligned}$$

$$\text{Since } v_t(0, t) = 0, \quad v_t(L, t) = 0$$

So, equation (2.3.5) becomes

$$\int_0^L {}_t^c D_{0+}^{1-\alpha} v(x, t) v_t(x, t) dx + \int_0^L v_{tx} v_x(x, t) dx = 0$$

Taking the integral from 0 to t_n with respect to t , then we have:

$$\int_0^{t_n} \int_0^L {}_t^c D_{0+}^{1-\alpha} v(x, t) v_t(x, t) dx dt + c \int_0^{t_n} \int_0^L v_{tx} v_x(x, t) dx dt = 0.$$

$$\int_0^{t_n} \int_0^L {}^C D_{0+}^{1-\alpha} v(x, t) v_t(x, t) dx dt + c \int_0^{t_n} \int_0^L v_{tx} v_x(x, t) dx dt = 0 .$$

$$\int_0^{t_n} \int_0^L {}^C D_{0+}^{1-\alpha} v(x, t) v_t(x, t) dx dt + \frac{c}{2} \int_0^L (v_x^2(x, t_n) - v_x^2(0, t_n)) dx = 0 .$$

The integral $\int_0^{t_n} \int_0^L {}^C D_{0+}^{1-\alpha} v(x, t) v_t(x, t) dx dt$ is positive because of coercivity inequality [42].

Since the first integral is positive and the second integral is also positive in the left hand side, then the sum of them equals zero.

implies that the first integral is zero and the second integral is zero

So, we have

$$v_x(x, t_n) = 0 ,$$

Integrate with respect to x, we get

$$\int_0^L v_x(x, t_n) dx = v(L, t_n) - v(0, t_n) = 0$$

Then $u_1 - u_2 = 0$,

So $u_1 = u_2$ then the solution is unique .

2.4 Analytic Solution of Fractional Convection -Diffusion

Equation.

This section presents the solution of the Fokker-Planck equation (1.1.1) when $0 < \alpha < 1$, $\beta = 1$, d and c are constants. Then the Fokker-Planck equation becomes:

$${}_t^c D_{0+}^{1-\alpha} u(x, t) = \frac{\partial u^{1-\alpha}}{\partial t^{1-\alpha}} = -d \frac{\partial u}{\partial x} + c \frac{\partial^2 u}{\partial x^2}$$

where $0 < \alpha < 1$

With $u(0, t) = A$, $u(L, t) = B$

$$u(x, 0) = f(x)$$

The characteristic equation is:

Let $v(x, t) = X(x)T(t)$

If $\lambda < 0$, then we ;

$$c \frac{X''(x)}{X(x)} - d \frac{X'(x)}{X(x)} = \frac{\partial T^\alpha}{T \partial t^\alpha} = \lambda$$

$$c \frac{X''(x)}{X(x)} - d \frac{X'(x)}{X(x)} = \lambda \text{ and } \frac{\partial u^\alpha}{\partial t^\alpha} = \lambda$$

Hence, X and T must satisfy

$$c\dot{X}(x) - d\dot{X}(x) - \lambda X(x) = 0 \tag{3.4.1}$$

$$\frac{\partial T^\alpha}{\partial t^\alpha} - \lambda T(t) = 0 \quad (3.4.2)$$

To solve equation (3.4.1), we use the same manner that we used in section (2.2)

To obtain

$$X_n(x) = B_n \sin\left(\frac{n\pi}{L}x\right)$$

To solve equation (3.4.2), we use the same manner that we used in section (2.3)

To get

$$T_n(t) = T(0) E_{1-\alpha,1}(-\lambda_n ct^{1-\alpha})$$

Hence, the nontrivial solution of the heat equation which satisfies the two

boundary conditions is $u_n(x, t) = a_n e^{\frac{dx}{2c}} E_{1-\alpha,1}(-\lambda_n ct^{1-\alpha}) \sin\left(\frac{n\pi}{L}x\right)$

where $a_n = B_n T(0)$ is an arbitrary constant.

By the principle of superposition, we obtain a formal series solution as

So,

$$v(x, t) = \sum_{n=0}^{\infty} X_n(x) T_n(t)$$

$$v(x, t) = \sum_{n=0}^{\infty} a_n e^{\frac{dx}{2c}} E_{1-\alpha,1}(-\lambda_n ct^{1-\alpha}) \sin\left(\frac{n\pi}{L}x\right)$$

which satisfies the initial condition if:

$$v(x, 0) = f(x) - G(x) = \sum_{n=0}^{\infty} a_n e^{\frac{dx}{2c}} E_{1-\alpha,1}(-\lambda_n ct^{1-\alpha}) \sin\left(\frac{n\pi}{L}x\right).$$

CHAPTER THREE

Numerical Solution of Fokker-Planck Equation

In dealing with many equations arising from the modelling of physical problems, the determination of such exact solutions in a simple domain is a hard task even when the boundary and/or initial data are simple. It is then necessary to resort to numerical solutions or approximation methods in order to deal with the problems that cannot be solved analytically. In view of the widespread accessibility of today's high speed electronic computers, numerical and approximation methods are becoming increasingly important and useful in applications. In particular, numerical solutions are also important in making initial guess of the exact solution. Thus, one can proceed with the analytical solution in parallel with the numerical approximate solution. Generally speaking, numerical solution involves the risk of convergence, thus extra care needed when choosing the algorithm and the step size, and it varies from one problem to the other.

In this chapter, we solve the Fokker-Planck equation using explicit finite difference method for some cases. Moreover, we investigate the stability for the numerical solution for the Fokker-Planck equation.

3.1 Explicit Finite Difference Method for Diffusion Equation.

In this section, we solve the Fokker -Plank equation (2.1.1) , $u_t = cu_{xx}$ by using explicit difference method [43]. Furthermore, we study the stability for the solution of equation (2.1.1).

First, We divide the interval $[0, T]$ into N subintervals with step size in time $k = \frac{T}{N}$. We also divide the interval $[0, L]$ into M subintervals with step size in size $h = \frac{L}{M}$. Next , we write the Taylor series for u in time about the point

(x_i, t_n) and evaluating at t_{n+1} later, then we have

$$u(x_i, t_{n+1}) = u(x_i, t_n) + ku_t(x_i, t_n) + \frac{k^2}{2}u_{tt}(c_i, d_n)$$

or

$$u_t(x_j, t_n) = \frac{u(x_j, t_{n+1}) - u(x_j, t_n)}{k} - \frac{k}{2}u_{tt}(c_j, d_n) \quad (3.1.1)$$

Expanding u in the third Taylor theorem in space about x_j and evaluating at x_{j+1} and at x_{j-1} and assuming $u \in C^4[x_{j-1}, x_{j+1}]$, then we obtain

$$u(x_{j+1}, t_n) = u(x_n, t_n) + hu_x(x_n, t_n) + \frac{h^2}{2}u_{xx}(x_n, t_n) + \frac{h^3}{6}u_{xxx}(x_n, t_n) + \frac{h^4}{(4)!}u_{xxxx}(c_{j+1}, d_n)$$

$$u(x_{j-1}, t_n) = u(x_j, t_n) - hu_x(x_j, t_n) + \frac{h^2}{2}u_{xx}(x_j, t_n) - \frac{h^3}{6}u_{xxx}(x_j, t_n) + \frac{h^4}{(4)!}u_{xxxx}(c_j, t_n)$$

$$u_{xx}(x_j, t_n) = \frac{1}{h^2}(u(x_{j+1}, t_n) - 2u(x_j, t_n) + u(x_{j-1}, t_n)) - \frac{h^2}{12}u_{xxxx}(c_j, t_n)$$

Assuming that U_j^n be approximate solution (numerical solution) for u at the point (x_j, t_n) .

After writing $u(x_{j+1}, t_n)$ as U_{j+1}^n and $u(x_{j-1}, t_n)$ as U_{j-1}^n , then we have

$$u_{xx}(x_j, t_n) = \left(\frac{U_{j+1}^n - 2U_j^n + U_{j-1}^n}{h^2} \right) - \frac{h^2}{12}u_{xxxx}(c_j, t_n) \quad (3.1.2)$$

$$c_j \in (x_{j-1}, x_{j+1})$$

Equation (3.1.2) is called second order centred difference formula in space.

Also, expanding u in the third Taylor theorem in space about x_j and evaluated x_{j+1} and x_{j-1} , then we have

$$u_x(x_j, t_n) = \frac{1}{2h}(u(x_{j+1}, t_n) - u(x_{j-1}, t_n)) - \frac{h^2}{3}u_{xxx}(c_j, t_n)$$

$$c_j \in (x_{j-1}, x_{j+1})$$

Substituting (3.1.1) and (3.1.2) in (2.1.1), then we have

$$\frac{U_j^{n+1} - U_j^n}{k} = c \left(\frac{U_{j+1}^n - 2U_j^n + U_{j-1}^n}{h^2} \right)$$

$$\text{Or } U_j^{n+1} = U_j^n + d(U_{j+1}^n - 2U_j^n + U_{j-1}^n) \quad (3.1.3)$$

Where $d = \frac{ck}{h^2}$ called the *diffusion number*.

Example (3.1.1): Solve the following PDE

$$u_t = 0.01 u_{xx} \quad , \quad 0 < x < 1 \quad , \quad t > 0$$

$$u(0, t) = 0 \quad , \quad t \geq 0$$

$$u(1, t) = 0 \quad , \quad t \geq 0$$

$$u(x, 0) = \begin{cases} 200x & \text{if } 0 < x < 0.5 \\ 200(1 - x) & \text{if } 0.5 \leq x < 1 \end{cases}$$

Consider $h = k = 0.1$.

Solution : Using formula (3.1.3) with $U_0^n = 0$ and $U_4^n = 0$ to obtain

$$U_j^{n+1} = U_j^n + d(U_{j+1}^n - 2U_j^n + U_{j-1}^n)$$

When $n=0$, we have

For $j=1$:

$$U_1^1 = U_1^0 + d(U_2^0 - 2U_1^0 + U_0^0)$$

$$U_1^1 = 200(0.1) + 0.1((0.2)(200) - 2(0.1)(200) + 0) = 20$$

For $j=2$:

$$U_2^1 = U_2^0 + d(U_3^0 - 2U_2^0 + U_1^0)$$

$$U_2^1 = 200(0.0.2) + 0.1((0.3)(200) - 2(0.2)(200) + (0.1)(200)) = 40$$

For j=3:

$$U_3^1 = U_3^0 + d(U_4^0 - 2U_3^0 + U_2^0) = 60$$

When n=1, we have

For j=1:

$$U_1^2 = U_1^1 + d(U_2^1 - 2U_1^1 + U_0^1)$$

$$U_1^2 = 20 + 0.1(40 - 40 + 0) = 20$$

For j=2:

$$U_2^2 = U_2^1 + d(U_3^1 - 2U_2^1 + U_1^1)$$

$$U_2^2 = 40 + 0.1(60 - 80 + 20) = 40$$

For j=3:

$$U_3^2 = u_3^1 + d(U_4^1 - 2U_3^1 + U_2^1)$$

$$U_3^2 = 60 + 0.1(0 - 120 + 40) = 52$$

When n=2, we have

For j=1:

$$U_1^3 = U_1^2 + d(U_2^2 - 2U_1^2 + U_0^2) = 19.9$$

For j=2:

$$U_2^3 = U_2^2 + d(U_3^2 - 2U_2^2 + U_1^2) = 39.2$$

For j=3:

$$U_3^3 = U_3^2 + d(U_4^2 - 2U_3^2 + U_2^2) = 45.6$$

When n=3, we have

For j=1:

$$U_1^4 = U_1^3 + d(U_2^3 - 2U_1^3 + U_0^3) = 19.9$$

For j=2:

$$U_2^4 = U_2^3 + d(U_3^3 - 2U_2^3 + U_1^3) = 37.9$$

For j=3:

$$U_3^4 = U_3^3 + d(U_4^3 - 2U_3^3 + U_2^3) = 40.4$$

By using Matlab code we get the following results that are showed in the following table

N	j	U_j^n
0	1	20
0	2	40
0	3	60
1	1	20
1	2	40
1	3	52
2	1	19.9
2	2	39.2
2	3	45.6
3	1	19.9
3	2	37.9
3	3	40.4

Example (3.1.2): Solve the following PDE by using finite difference method

$$u_t = 0.001 u_{xx} \quad , \quad 0 < x < 1 \quad , \quad t > 0$$

$$u(0, t) = 0 \quad , \quad t \geq 0$$

$$u(1, t) = 0 \quad , \quad t \geq 0$$

$$u(x, 0) = \begin{cases} 200x & \text{if } 0 < x < 0.5 \\ 200(1 - x) & \text{if } 0.5 \leq x < 1 \end{cases}$$

Consider $h = k = 0.04$.

Solution : Using formula (3.1.3) with $U_0^n = 0$ and $U_{25}^n = 0$ to obtain

$$U_j^{n+1} = U_j^n + d(U_{j+1}^n - 2U_j^n + U_{j-1}^n)$$

When $n=0$, we have

For $j=1$:

$$U_1^1 = U_1^0 + d(U_2^0 - 2U_1^0 + U_0^0)$$

$$U_1^1 = 200(0.04) + 0.25((0.08)(200) - 2(0.04)(200) + 0) = 8$$

For $j=2$:

$$U_2^1 = U_2^0 + d(U_3^0 - 2U_2^0 + U_1^0)$$

$$U_2^1 = 200(0.08) + 0.25((0.12)(200) - 2(0.08)(200) + (0.04)(200)) = 16$$

For $j=3$:

$$U_3^1 = U_3^0 + d(U_4^0 - 2U_3^0 + U_2^0) = 24$$

When $n=1$, we have

For $j=1$:

$$U_1^2 = U_1^1 + d(U_2^1 - 2U_1^1 + U_0^1) = 8$$

For $j=2$:

$$U_2^2 = U_2^1 + d(U_3^1 - 2U_2^1 + U_1^1) = 16$$

For $j=3$:

$$U_3^2 = U_3^1 + d(U_4^1 - 2U_3^1 + U_2^1)$$

$$U_3^2 = 60 + 0.1(0 - 120 + 40) = 24$$

When n=2, we have

For j=1:

$$U_1^3 = U_1^2 + d(U_2^2 - 2U_1^2 + U_0^2) = 8$$

For j=2:

$$U_2^3 = U_2^2 + d(U_3^2 - 2U_2^2 + U_1^2) = 16$$

For j=3:

$$U_3^3 = U_3^2 + d(U_4^2 - 2U_3^2 + U_2^2) = 24$$

When n=3, we have

For j=1:

$$U_1^4 = U_1^3 + d(U_2^3 - 2U_1^3 + U_0^3) = 8$$

For j=2:

$$U_2^4 = U_2^3 + d(U_3^3 - 2U_2^3 + U_1^3) = 16$$

For j=3:

$$U_3^4 = U_3^3 + d(U_4^3 - 2U_3^3 + U_2^3) = 24$$

The following table summarize the results above generated using Matlab code

The approximate solution (U_j^n)											
N	j=0	j=1	j=2	j=3	j=4	j=5	j=6	j=7	j=8	j=9	j=10
0	0	8	16	24	32	40	48	56	46	72	80
1	0	8	16	24	32	40	48	56	64	72	80
5	0	8	16	24	32	40	48	56	64	72	80
10	0	8	16	24	32	40	48	56	64	71.999	79.988
20	0	8	16	24	32	40	48	56	63.999	71.991	79.914
25	0	8	16	24	32	40	48	56	63.999	71.985	79.876

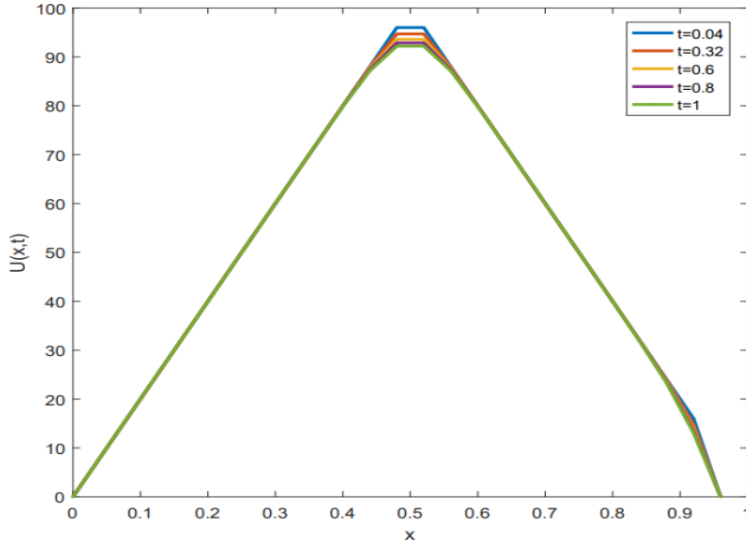


Figure (3.1.1): Numerical solution of one dimensional heat equation (3.1.1) with $c = 0.001 \text{ cm}^2 / \text{s}$ for different time mesh gratings.

The next theorem shows the approximate solution of equation (3.1.3) is conditionally stable.

Theorem (3.1.1) [30] : The approximate solution for equation (3.1.3) is conditionally stable.

Proof: To show that the stability, we use complex Fourier series for

$u(x, t_n) = F(x)$ is given by

$$u(x, t_n) = F(x) = \sum_{m=-\infty}^{\infty} c_m e^{ik_m x} = \sum_{m=-\infty}^{\infty} F_m$$

Where $k_m = \frac{m\pi}{L}$

Let $u_j^n = u(x_j, t_n)$ consists of the general term U_m . Thus,

$$u_j^n = F_m = c_m e^{ik_m x_j} = c_m e^{i(jhk_m)}$$

$$u_{j+1}^n = F_m = c_m e^{ik_m x_{j+1}} = c_m e^{i(jhk_m)} e^{i(hk_m)} = U_j^n e^{i(hk_m)}$$

so, equation (3.1.3) becomes

$$u_j^{n+1} = u_j^n + d(u_j^n e^{i\theta} - 2u_j^n + u_j^n e^{-i\theta}) = u_j^n(1 + 2d(\cos\theta - 1))$$

$$\text{So , } G = 1 + 2d(\cos\theta - 1)$$

$$|G| \leq 1$$

$$-1 \leq 1 + 2d(\cos\theta - 1) \leq 1$$

$$-1 \leq d(\cos\theta - 1) \leq 0$$

$$\frac{-1}{d} + 1 \leq (\cos\theta) \leq 1$$

Thus,

$$|G| \leq 1 \text{ for all values of } \theta = hk_m \text{ if } d \leq \frac{1}{2}$$

Hence, the numerical solution is conditionally stable.

Example (3.1.3): Investigate the stability for the numerical solution of the following equation

$$u_t = 0.001 u_{xx} \quad , \quad 0 < x < 1 \quad , \quad t > 0$$

$$u(0, t) = 0 \quad , \quad t \geq 0 \quad , \quad u(1, t) = 0 \quad , \quad t \geq 0$$

$$u(x, 0) = \begin{cases} 200x & \text{if } 0 < x < 0.5 \\ 200(1 - x) & \text{if } 0.5 \leq x < 1 \end{cases}$$

Consider $h = k = 0.04$.

Solution: The approximate solution is conditionally stable since

$$d = \frac{ck}{h^2} = \frac{(0.001)(0.04)}{(0.04)^2} = 0.025 < 0.5$$

Example (3.1.4): Investigate the stability for the numerical solution of the following equation

$$u_t = 0.1 u_{xx} \quad , \quad 0 < x < 1 \quad , \quad t > 0$$

$$u(0, t) = 0 \quad , \quad t \geq 0$$

$$u(1, t) = 0 \quad , \quad t \geq 0$$

$$u(x, 0) = \begin{cases} 200x & \text{if } 0 < x < 0.5 \\ 200(1-x) & \text{if } 0.5 \leq x < 1 \end{cases}$$

Consider $k = 0.4$, $h = 0.1$

Solution: The approximate solution is not conditionally stable since

$$d = \frac{ck}{h^2} = \frac{(0.1)(0.4)}{(0.1)^2} = 4 \text{ (which is not less than 0.5)}$$

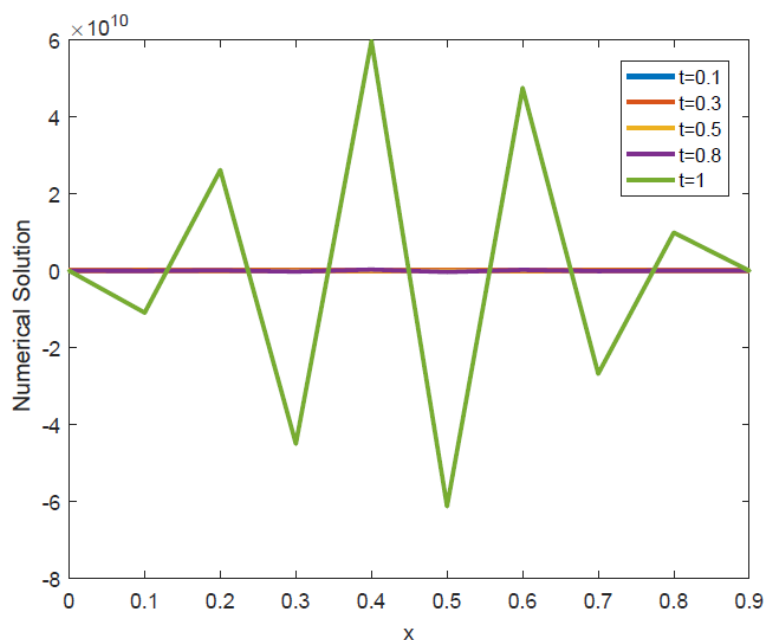


Figure (3.1.2): Numerical solution for example (3.1.4) which is not conditionally stable as explained in the main text.

3.2 Explicit Finite Difference Method for Convection -Diffusion

Equation.

In this section we want to solve Fokker-Planck equation (2.2.1),

$$U_t = -d U_x + cU_{xx}$$

By using explicit finite difference method in time and finite difference in space

and follow the same steps that we used in section (3.1), then we have

$$\frac{U_j^{n+1} - U_j^n}{k} = -d \left(\frac{U_{j+1}^n - U_{j-1}^n}{2h} \right) + c \left(\frac{U_{j+1}^n - 2U_j^n + U_{j-1}^n}{h^2} \right)$$

$$\frac{U_j^{n+1}}{k} = \frac{U_j^n}{k} - \frac{2c U_j^n}{h^2} - \frac{d U_{j+1}^n}{2h} + \frac{c U_{j+1}^n}{h^2} + \frac{d U_{j-1}^n}{2h} + \frac{c U_{j-1}^n}{h^2}$$

Multiply both sides by k we get:

$$U_j^{n+1} = U_j^n - \frac{2c k U_j^n}{h^2} - \frac{d k U_{j+1}^n}{2h} + \frac{c k U_{j+1}^n}{h^2} + \frac{d k U_{j-1}^n}{2h} + \frac{c k U_{j-1}^n}{h^2}$$

$$U_j^{n+1} = \left(\frac{ck}{h^2} + \frac{d k}{2h} \right) U_{j-1}^n + \left(1 - \frac{2c k}{h^2} \right) U_j^n + \left(\frac{ck}{h^2} - \frac{d k}{2h} \right) U_{j+1}^n \quad (3.2.1)$$

$$\begin{bmatrix} U_1^{n+1} \\ U_2^{n+1} \\ \vdots \\ U_n^{n+1} \end{bmatrix} = \begin{bmatrix} A & B & C & 0 & 0 \\ 0 & A & B & C & 0 \\ 0 & 0 & A & B & C \end{bmatrix} \begin{bmatrix} U_0^n \\ U_1^n \\ \vdots \\ U_{m-1}^n \end{bmatrix}$$

Where $A = \frac{ck}{h^2} + \frac{d k}{2h}$.

$$B = 1 - \frac{2c k}{h^2}$$

$$C = \frac{ck}{h^2} - \frac{dk}{2h}$$

Example (3.2.1): Solve the following PDE by using explicit finite difference method

$$u_t = -0.1u_x + c u_{xx} \quad , \quad 0 < x < 1 \quad , \quad t > 0$$

$$u(0, t) = 0 \quad , \quad t \geq 0$$

$$u(1, t) = 100 \quad , \quad t \geq 0$$

$$u(x, 0) = 100x$$

Consider $h = k = 0.04$.

Solution: using the numerical formula (3.2.1) we get,

When $n=0$,

For $j = 1$,

$$U_1^1 = 100 (0.04) = 4$$

For $j=2$;

$$U_1^2 = 100(0.08) = 8$$

For $j = 3$;

$$U_1^3 = 100 (0.12) = 12$$

For $j = 4$;

$$U_1^4 = 100(0.16) = 16$$

When n= 1;

For j= 1;

$$U_1^2 = \left(\frac{0.01 \times 0.04}{0.04^2} - \frac{0.1 \times 0.04}{2 \times 0.04} \right) U_0^1 + \left(1 - \frac{2 \times 0.01 \times 0.04}{0.04^2} \right) U_1^1 +$$

$$\left(\frac{0.01 \times 0.04}{0.04^2} - \frac{0.1 \times 0.04}{2 \times 0.04} \right) U_2^1$$

$$= (0.3) 0 + (0.5) 4 + (0.25 - 0.05) 8 =$$

$$= 2 + 1.6 = 3.6.$$

For j= 2

$$U_2^2 = (0.3)U_1^1 + 0.5 U_2^1 + 0.2 U_3^1$$

$$= (0.3) \times 4 + 0.5 \times 8 + 0.2 (100) \times 0.12 =$$

$$= 7.6.$$

For j=3;

$$U_3^2 = 0.3 U_2^1 + 0.5 U_3^1 + 0.2 U_4^1 = 11.6$$

For j= 4

$$U_4^2 = 0.3 U_3^1 + 0.5 U_4^1 + 0.2 U_5^1 = 15.6$$

When n= 2 ;

For j= 1 ;

$$U_1^3 = (0.3)U_0^2 + 0.5 U_1^2 + 0.2 U_2^2$$

$$= 0.3 \times 0 + 0.5 \times 3.6 + 0.2 \times 7.6 = 3.32$$

For j=2

$$U_2^3 = 0.3 U_1^2 + 0.5 U_2^2 + 0.2 U_3^2 = 7.2$$

The tables below show the results for several iterations

The approximate solution(U_j^n) , c=0.01, M=N=10										
n	j=0	j=1	j=2	j=3	j=4	j=5	j=6	j=7	j=8	j=9
0	0	4	8	12	16	20	24	28	32	100
1	0	3.6	7.6	11.6	15.2	19.6	23.6	27.6	44.4	100
5	0	2.7602	6.2113	10.038	14.024	18.308	24.151	35.336	85.471	100
9	0	2.2883	5.2649	8.8001	12.904	18.092	25.897	39.275	62.436	100

The approximate solution(U_j^n) , c=0.001, M=N=10										
n	j=0	j=1	j=2	j=3	j=4	j=5	j=6	j=7	j=8	j=9
0	0	4	8	12	16	20	24	28	32	100
1	0	3.6	7.6	11.6	15.2	19.6	23.6	27.6	30	100
5	0	2.2851	6.0214	10.001	14	18	21.991	26.363	22.694	100
9	0	1.3569	4.5618	8.4182	12.401	16.403	20.333	25.542	16.448	100

The following figure represents the numerical solution for equation (3.2.1)

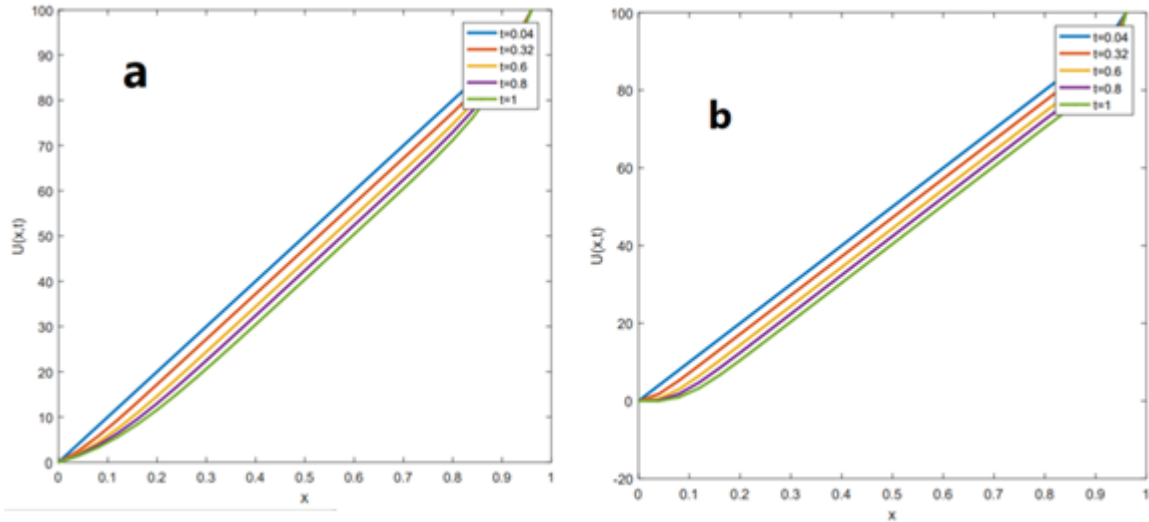


Figure (3.2.1): Numerical solution of convection-diffusion equation. Part(a), represents the solution with $c = 0.01 \text{ cm}^2 / \text{s}$ for different time mesh gradings. Part(b), represents the numerical solution of convection-diffusion equation with $c = 0.001 \text{ cm}^2 / \text{s}$ for different time mesh gradings.

Next, we will study the stability of the approximate solution for equation (3.2.1).

Theorem (3.2.1) [30]: The approximate solution for equation (3.2.1) is conditionally stable.

$u(x, t_n) = F(x)$ is given by

$$u(x, t_n) = F(x) = \sum_{m=-\infty}^{\infty} c_m e^{ik_m x} = \sum_{m=-\infty}^{\infty} F_m(x)$$

Where $k_m = \frac{m\pi}{L}$.

Let $U_j^n = u(x_j, t_n)$ consists of the general term F_m .

Thus,

$$U_j^n = F_m(x_j) = c_m e^{ik_m x_j} = c_m e^{i(jhk_m)}$$

$$U_{j+1}^n = F_m(x_{j+1}) = c_m e^{ik_m x_{j+1}} = c_m e^{i(jhk_m)} e^{i(hk_m)} = U_j^n e^{i(hk_m)}$$

So, (equation 3.2.1) becomes:

$$U_j^{n+1} = U_j^n - \frac{k d}{2h} (U_{j+1}^n - U_{j-1}^n) + \frac{ck}{h^2} (U_{j+1}^n - 2 U_j^n + U_{j-1}^n)$$

$$U_j^{n+1} = U_j^n - \frac{k d}{2h} (U_j^n e^{i\theta} - U_j^n e^{-i\theta}) + \frac{ck}{h^2} (U_j^n e^{i\theta} - 2 U_j^n + U_j^n e^{-i\theta})$$

$$U_j^{n+1} = U_j^n - \frac{k d}{2h} \left(\frac{e^{i\theta} - e^{-i\theta}}{2} \right) U_j^n + \frac{ck}{h^2} \left(\frac{e^{i\theta} - e^{-i\theta} - 2}{2} \right) U_j^n.$$

$$U_j^{n+1} = U_j^n - \frac{k d}{2h} \left(\frac{e^{i\theta} - e^{-i\theta}}{2} \right) U_j^n + \frac{ck}{h^2} \left(\frac{e^{i\theta} - e^{-i\theta} - 2}{2} \right) U_j^n.$$

By using $\cos\theta = \frac{e^{i\theta} + e^{-i\theta}}{2}$, $= \frac{e^{i\theta} - e^{-i\theta}}{2i}$, then we have :

$$U_j^{n+1} = \left(1 - i \frac{k d}{2h} \sin \theta + \frac{2 c k}{h^2} \cos \theta - \frac{2 c k}{h^2} \right) U_j^n.$$

Letting $C = \frac{k d}{h}$, $D = \frac{c k}{h^2}$, then we obtain

$$U_j^{n+1} = \left(1 - 2D + 2D \cos \theta - i \frac{C}{2} \sin \theta \right) U_j^n$$

$$\text{Letting } G = 1 - 2D + 2D \cos \theta - i \frac{C}{2} \sin \theta \quad (3.2.2)$$

Equation (3.2.2) represents an ellipse in the complex plane.

The real and imaginary axes of the ellipse must both be less than or equal to unity ($|G| \leq 1$)

From this, we have

$$C \leq 1 \quad \text{and} \quad 2D \leq 1$$

In addition, at point $(1 + i0)$ the curvature of the ellipse must be greater than the curvature of the Unit circle, or the ellipse will not remain within the Unit circle even though $C \leq 1$ and $D \leq 1/2$. This condition is satisfied if:

$$C^2 \leq 2D \leq 1.$$

3.3 Explicit Finite Difference Method for Fractional Diffusion

Equation.

In this section we want to solve Fokker-Planck equation (2.3.1),

$${}_t^c D_{0+}^{1-\alpha} u = cu_{xx}$$

Where ${}_t^c D_{0+}^{1-\alpha} u(t) = I^\alpha \dot{u}(t) = \int_0^t (t-s)^{\alpha-1} \dot{u}(s) ds$.

By using explicit finite difference method [58], then we get

$$I^\alpha \dot{u}(t_n) = \frac{1}{\Gamma(\alpha)} \int_0^{t_n} (t_n - s)^{\alpha-1} u'(s) ds$$

$$I^\alpha u'(t_n) = \sum_{i=1}^n \int_{t_{i-1}}^{t_i} \frac{(t_n - s)^{\alpha-1}}{\Gamma(\alpha)} \frac{(u(t_i) - u(t_{i-1}))}{k_i} ds$$

$$I^\alpha u'(t_n) = \sum_{i=1}^n \frac{(u(t_i) - u(t_{i-1}))}{k_i} \frac{((t_n - t_{i-1})^\alpha - (t_n - t_i)^\alpha)}{\Gamma(\alpha + 1)}$$

Or

$$\begin{aligned}
I^\alpha u'(t_n) &= u(t_n) \frac{((t_n - t_{n-1}))^\alpha}{k_1 \Gamma(\alpha + 1)} + u(t_0) \frac{((t_n - t_0)^\alpha - (t_n - t_1)^\alpha)}{k_1 \Gamma(\alpha + 1)} \\
&\quad + \sum_{i=1}^{n-1} u(t_i) \left(\frac{((t_n - t_{i-1}))^\alpha - (t_n - t_i)^\alpha}{k_{i+1} \Gamma(\alpha + 1)} \right. \\
&\quad \left. - \frac{((t_n - t_i)^\alpha - (t_n - t_{i+1}))^\alpha}{k_i \Gamma(\alpha + 1)} \right)
\end{aligned}$$

$$a_n = (n + 1)^\alpha - n^\alpha$$

$$I^\alpha u'(t_n) = \frac{k^{\alpha-1}}{\Gamma(\alpha + 1)} \left[a_0 u(t_n) - u(t_0) a_{n-1} - \sum_{i=1}^{n-1} u(t_i) (a_{n-i-1} - a_{n-i}) \right]$$

$$\begin{aligned}
I^\alpha u'(t_n) &= \frac{k_n^{-1+\alpha}}{\Gamma(\alpha + 1)} (u(t_n) - u(t_{n-1})) \\
&\quad + \sum_{i=1}^{n-1} \frac{(u(t_i) - u(t_{i-1})) ((t_n - t_{i-1}))^\alpha - (t_n - t_i)^\alpha)}{k_i \Gamma(\alpha + 1)}
\end{aligned}$$

$$\begin{aligned}
U_j^n &= a_{n-1} U_j^0 + \frac{\Gamma(\alpha + 1) k_n^{1-\alpha} c}{h^2} (U_{j+1}^{n-1} - 2U_j^{n-1} + U_{j-1}^{n-1}) \\
&\quad + \sum_{r=1}^{n-1} U_j^{r-1} (a_{n-i-1} - a_{n-i})
\end{aligned}$$

$$U_j^n = a_{n-1} U_j^0 + g (U_{j+1}^{n-1} - 2U_j^{n-1} + U_{j-1}^{n-1}) + \sum_{r=1}^{n-1} U_j^{r-1} (a_{n-i-1} - a_{n-i})$$

$$\text{Where } g = \frac{\Gamma(\alpha+1) k_n^{1-\alpha} c}{h^2}$$

Or

$$\begin{aligned}
 U_j^n = & k_n^{\alpha-1} U(t_0) \frac{((t_n - t_0)^\alpha - (t_n - t_1)^\alpha)}{k_1} \\
 & + \frac{\Gamma(\alpha + 1) k_n^{1-\alpha} c}{h^2} (U_{j+1}^{n-1} - 2U_j^{n-1} + U_{j-1}^{n-1}) \\
 & - k_n^{\alpha-1} \sum_{i=1}^{n-1} U_j^i \left(\frac{((t_n - t_{i-1})^\alpha - (t_n - t_i)^\alpha)}{k_{i+1}} - \frac{((t_n - t_i)^\alpha - (t_n - t_{i+1})^\alpha)}{k_i} \right)
 \end{aligned}
 \tag{3.3.1}$$

Example(3.3.1): Use explicit finite difference method to solve the following equation

$${}^c D_{0+}^{1-\alpha} u = cu_{xx}$$

$$u(0, t) = 0, \quad t \geq 0$$

$$u(1, t) = 0, \quad t \geq 0$$

$$u(x, 0) = \begin{cases} 200x & \text{if } 0 < x < 0.5 \\ 200(1-x) & \text{if } 0.5 \leq x < 1 \end{cases}$$

Consider $h = k = 0.04$.

Solution:

Using the following formula:

$$U_j^n = a_{n-1} U_j^0 + g(U_{j+1}^{n-1} - 2U_j^{n-1} + U_{j-1}^{n-1}) + \sum_{r=1}^{n-1} U_j^{r-1} (a_{n-i-1} - a_{n-i})$$

$$\text{Where } g = \frac{\Gamma(\alpha+1)k_n^{1-\alpha}c}{h^2}.$$

and

$$a_n = (n + 1)^\alpha - n^\alpha, \alpha = 0.3, c = 0.001.$$

When $n = 1$;

For $j = 1$;

$$U_1^1 = a_0 U_1^0 + g(U_2^0 - 2 U_1^0 + U_0^0)$$

$$a_0 = (0 + 1)^{0.3} - 0^{0.3} = 1.$$

$$g = \frac{\Gamma(0.3 + 1)(0.04)^{1-0.3}(0.001)}{(0.004)^2} = 0.00589$$

$$U_1^1 = 1(8) + 0.00589(16 - 2(8) + 0) = 8$$

For $j = 2$;

$$U_2^1 = a_0 U_1^0 + g(3 - 2 U_2^0 + U_1^0).$$

$$= 1(16) + 0.00589(24 - 2(16) + 8) = 16.$$

For $j = 3$;

$$U_3^1 = a_0 U_3^0 + g(U_4^0 - 2 U_3^0 + U_2^0)$$

$$= 1(24) + 0.00589(32 - 2(24) + 16) = 24.$$

For $j = 4$

$$U_4^1 = a_0 U_4^0 + g(U_5^0 - 2 U_4^0 + U_3^0) = 32$$

When $n= 2$;

For $j= 1$;

$$U_j^2 = a_1 U_j^0 + g(U_{j+1}^1 - 2 U_j^1 + U_{j-1}^1) + U_j^0 (a_0 - a_1)$$

$$a_1 = 2^{0.3} - 1^{0.3} = 0.23114$$

$$U_1^2 = 0.23114 U_1^0 + 0.00589(U_2^1 - 2 U_1^1 + U_0^1) + U_1^0 (1 - 0.23114)$$

$$= 0.23114 (8) + 0.00589 (16 - 2 (8) + 0) + 8 (0.76886) .$$

$$= 8$$

For $j=2$;

$$U_2^2 = 0.23114 U_2^0 + 0.00589(U_3^1 - 2 U_2^1 + U_1^1) + U_2^0 (1 - 0.23114)$$

$$= 16.$$

For $j= 3$;

$$U_3^2 = 0.23114 U_3^0 + 0.00589(U_4^1 - 2 U_3^1 + U_2^1) + U_3^0 (0.76886)$$

$$= 24.$$

When $n= 3$;

For $j= 1$;

$$U_j^3 = a_2 U_j^0 + g(U_{j+1}^2 - 2 U_j^2 + U_{j-1}^2) + U_j^0 (a_0 - a_1) + U_j^1 (a_1 - a_2)$$

$$\text{Now } a_2 = 3^{0.3} - 2^{0.3} = 0.15924$$

$$U_j^2 = a_2 U_j^0 + g(U_{j+1}^1 - 2 U_j^1 + U_{j-1}^1) + U_j^0 (a_0 - a_1) + U_j^1 (a_1 - a_2)$$

$$U_1^3 = 0.15924 (U_1^0) + 0.00589(U_2^2 - 2 U_1^2 + U_0^2) + U_1^0 (0.76886) + U_1^1 (0.0719).$$

$$= 0.15924 (8) + 0.00589 (16 - 2 (8) + 0) + 8 (0.76886) + 8 (0.0719).$$

$$= 8.$$

For j = 2;

$$U_2^3 = 0.15924 (U_2^0) + 0.00589(U_3^2 - 2 U_2^2 + U_1^2) + U_2^0 (0.76886) + U_2^1 (0.0719).$$

$$= 16.$$

For j= 3;

$$U_3^3 = 0.15924 (U_3^0) + 0.00589(U_4^2 - 2 U_3^2 + U_2^2) + U_3^0 (0.76886) + U_3^1 (0.0719).$$

$$= 24.$$

By using MATLAB code , we get the following results that are shown in the table

The approximate solution(U_j^n), $M=N=10$										
n	j=0	j=1	j=2	j=3	j=4	j=5	j=6	j=7	j=8	j=9
0	0	8	16	24	32	40	48	56	64	0
1	0	8	16	24	32	40	48	56	59.757	100
5	0	8	16	24	32	39.999	47.916	54.701	51.65	100
9	0	8	16	24	31.998	39.970	47.666	52.234	47.190	100

The following figure represents the numerical solution for equation (3.3.1).

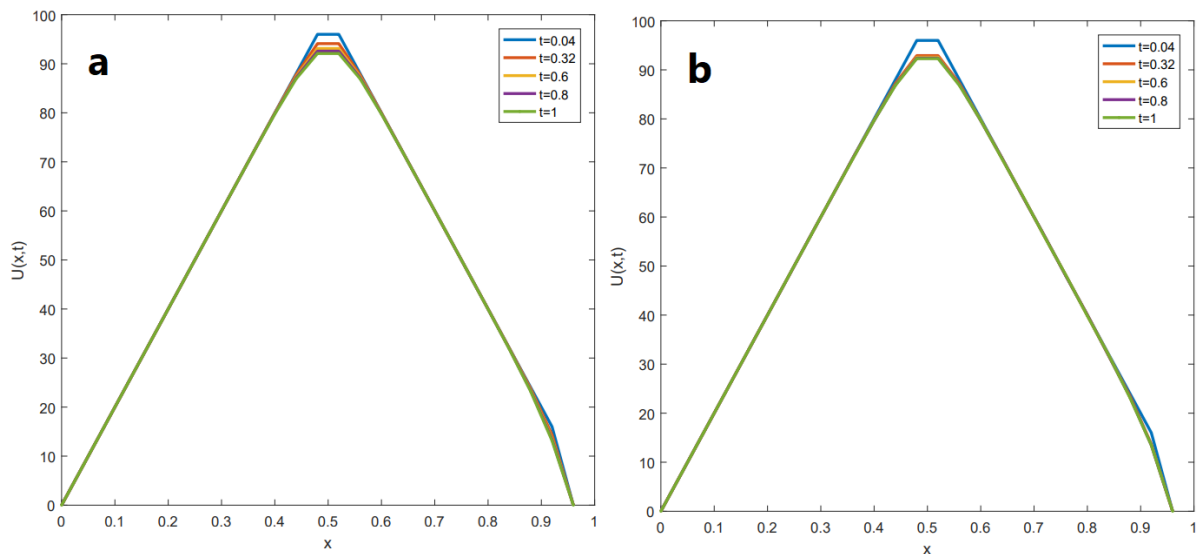


Figure (3.3.1): Numerical solution of fractional heat equation for different time mesh gradings with $\alpha = 0.3$ and $c = 0.001$ in part (a). $\alpha = 0.8$ and $c = 0.001$ in part (b).

Remark: If we look at the fractional heat equation with Neumann boundary condition, then the numerical solution admits following figure

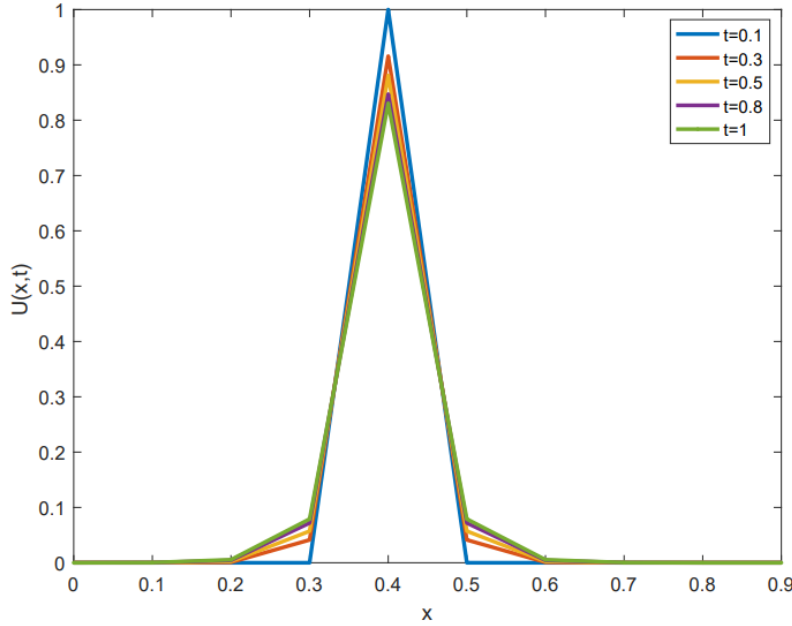


Figure (3.3.2) Numerical solution of fractional diffusion equation with Neumann boundary condition and the initial condition $u(x, 0) = 0$ every where except at $x = 1, u(1,0) = 1$, with $\alpha = 0.5$ and $M=N= 10$ for different time mesh gradings.

Next, we want to show that the approximate solution of equation (3.3.1) is conditionally stable.

Theorem (3.3.1): The approximate solution for equation (3.3.1) is conditionally stable.

Proof:

$$\text{Let } U_j^n = d_n e^{ijh\beta}, \beta = \frac{2\pi}{l}, d_n \geq 0$$

$$d_n e^{ijh\beta} = a_{n-1}d_0 e^{ijh\beta} + g d_{n-1} e^{i(j+1)h\beta} - 2 d_{n-1} e^{ijh\beta} + g d_{n-1} e^{i(j-1)h\beta} + \sum_{r=1}^{n-1} d_r e^{ijh\beta} (a_{n-r-1} - a_{n-r})$$

$$d_n = a_{n-1}d_0 + 2g d_{n-1} \cos\beta h - 2g d_{n-1} + \sum_{r=1}^{n-1} d_r (a_{n-r-1} - a_{n-r})$$

We want to show that $d_n \leq d_0$ for all $n \in N$ if

$$|a_0 + 2g \cos\beta h - 2g| \leq 1$$

For $n = 1$,

$$\begin{aligned} d_1 &= a_0 d_0 + 2g d_0 \cos\beta h - 2g d_0 \\ &= (a_0 + 2g \cos\beta h - 2g) d_0 \end{aligned}$$

So, $d_1 \leq (1)d_0 \leq d_0$

For $n = 2$,

$$\begin{aligned} d_2 &= a_1 d_0 + 2g d_1 \cos\beta h - 2g d_1 + d_1 (a_0 - a_1) \\ d_2 &\leq a_1 d_0 + 2g d_0 \cos\beta h - 2g d_0 + d_0 (a_0 - a_1) \\ d_2 &\leq a_0 d_0 + 2g d_0 \cos\beta h - 2g d_0 \\ d_2 &\leq d_0 \end{aligned}$$

Since $|a_0 + 2g \cos\beta h - 2g| < 1$, then we have :

$$d_2 \leq (1)d_0$$

Assume that when $n = k$ the statement is true

$$d_k \leq d_0$$

We want to show that the statement is true when $n = k + 1$

or

$$d_{k+1} \leq d_0$$

$$d_{k+1} = a_k d_0 + 2g d_k \cos \beta h - 2g d_k + \sum_{r=1}^k d_r (a_{n-r-1} - a_{n-r})$$

$$d_{k+1} \leq a_k d_0 + 2g d_0 \cos \beta h - 2g d_0 + \sum_{r=1}^k (a_{k-r} - a_{k-r+1}) d_0$$

$$d_{k+1} \leq (a_k + 2g d_k \cos \beta h - 2g + (a_0 - a_k)) d_0$$

$$d_{k+1} \leq (a_k + 2g d_k \cos \beta h - 2g) d_0$$

Since $|a_k + 2g d_k \cos \beta h - 2g| \leq 1$, then we have

$$d_{k+1} \leq d_0.$$

Hence, the approximate solution is conditionally stable.

3.4 Explicit Finite Difference Method for Fractional Convection - Diffusion Equation.

In this section we want to solve Fokker-Planck equation (2.3.1),

$${}_t^C D_{0+}^{1-\alpha} u(x, t) = -d u_x(x, t) + c u_{xx}(x, t)$$

by using Explicit Finite Difference Method.

Following the same manner that we used in sections (3.2) and (3.3), then we obtain

$$U_j^n = a_{n-1} U_j^0 - r(U_{j+1}^{n-1} - U_{j-1}^{n-1}) + g(U_{j+1}^{n-1} - 2U_j^{n-1} + U_{j-1}^{n-1}) +$$

$$\sum_{r=1}^{n-1} U_j^{r-1} (a_{n-r-1} - a_{n-r})$$

Where $g = \frac{\Gamma(\alpha+1)k_n^{1-\alpha}c^2}{h^2}$, $r = d \frac{\Gamma(\alpha+1)k_n^{1-\alpha}}{2h}$

Or

$$\begin{aligned} U_j^n &= a_{n-1}U(t_0) \frac{((t_n - t_0)^\alpha - (t_n - t_1)^\alpha)}{k_1} - r(U_{j+1}^{n-1} - U_{j-1}^{n-1}) \\ &\quad + \frac{\Gamma(\alpha + 1)k_n^{1-\alpha}c^2}{h^2} (U_{j+1}^{n-1} - 2U_j^{n-1} + U_{j-1}^{n-1}) \\ &\quad - k_n^{1-\alpha} \sum_{i=1}^{n-1} U_j^i \left(\frac{((t_n - t_{i-1})^\alpha - (t_n - t_i)^\alpha)}{k_{i+1}} - \frac{((t_n - t_i)^\alpha - (t_n - t_{i+1})^\alpha)}{k_i} \right) \end{aligned} \tag{3.3.2}$$

Remark: In this stage , we would like to mention that equation (2.1.1) and equation (2.2.2) can be solved numerically if the coefficient (c) of u_{xx} is time and position dependent ($c = c(x,t)$) and the coefficient (d) of u_x ($d = d(x, t)$) depends on x ,t .

CHAPTER FOUR

Stochastic Picture of Diffusion Equation

Stochastic process is a process in which a random step is taken. Stochastic approach is very fundamental in studying physical problem which involve randomness [21]. These processes appear in many real word problems such as in physics, biology [1; 2; 20], finance [51] and laser physics, in addition to semiconductor science [7] and chemistry [15]. The importance of studying the stochastic nature of these problems is due to the unknown physical mechanisms underlying these processes, hence, using a generalized noise term which has certain statistical nature can lump such hidden factors, yet gives a reasonable result which agrees with the experimentally observed phenomenon [21].

4.1 General Treatment.

In physics and many other fields, usually hidden factors and underlying processes are temperature dependent, hence, the noise usually have a temperature dependence [4; 19; 36]; for example the noise manifested in the motion of pollen grains in water, or ink molecules in water is driven by temperature. A reasonable and widely used approximation would be a Gaussian white noise ($\eta(t)$) whose intensity is temperature dependent, and uncorrelated in time [53]: its value at one instant of time is independent from its value at later or previous instants as long as the time difference between the two instants is

larger than some system specific value (τ_s) [6; 41]. Thus the mean of this noise is $\langle \eta(t) \rangle = 0$, where $\langle \dots \rangle$ indicates the ensemble average. Its autocorrelation function is given by

$\langle \eta(s) \eta(\tau) \rangle = \delta(s - \tau)$ [13], thus it is called a delta correlated Gaussian white noise, where s and τ are two different instants of time.

A specific type of the stochastic processes is the Markov process; the output of this process at the next time step doesn't depend on the previous history of the process but depends on the current state only [15]. This process is proved to be useful in modelling many physical systems and has wide application in many fields. Luckily the computation of this process are shown to be easier than those processes which has a memory kernel involved in them [14; 37].

Here, in this thesis we treat a diffusion problem on two different levels, one using the microscopic picture which is the Markov process view, and compared the results with the macroscopic view using the Fokker Plank equation which has been solved in different forms for generalized initial and boundary conditions in Chapter 2 and 3. In particular, we study the Brownian motion related to molecules (for clarity we will talk about ink molecules) diffuse in a fluid. This fluid has frictional forces and its molecules are moving in random directions which in role, generate a small kicks on the ink molecule. Using a simple form of Newton's second law, one can write the following equation [27]:

$m\ddot{x} = -\gamma\dot{x} + \text{Random Force generated by fluid molecules.}$

Since, the mass of the ink molecules is large compared to that of water molecules, we can ignore the term on the left as the acceleration is very small [27]. Thus, operating in the overdamped limit of the motion. The Random force can be modelled with Gaussian white noise, which has a zero mean and noise intensity D_0 ; hence

$$\dot{x} = \sqrt{2D_0} \eta(t) \quad (4.1.1)$$

This is a process known as wiener process in one dimension and it is a Markov process by definition [27; 54; 55]. Here and below we will call $D_0 = \sqrt{\frac{k_B T}{\gamma}}$ is the noise intensity [13]. where, γ is the viscosity coefficient (related to friction) in the fluid, k_B is the Boltzmann constant ($k_B = 1.38 \times 10^{-23}$ J/K), and T is the temperature of the medium.

One can easily show that the average of this process is zero, and its variance is given by

$$\dot{x} = \sqrt{2D_0} \eta(t)$$

$$x = x_0 + \sqrt{2D_0} \int_0^t \eta(s) ds.$$

$$x^2 = x_0^2 + 2\sqrt{2D_0}x_0 \int_0^t \eta(s) ds + 2D_0 \int_0^t \int_0^t \eta(s) \eta(\tau) ds d\tau.$$

$$\langle x^2 \rangle = \langle x_0^2 \rangle + 2x_0 \sqrt{2D_0} \int_0^t \langle \eta(s) \rangle ds + 2D_0 \int_0^t \int_0^t \langle \eta(s) \eta(\tau) \rangle ds d\tau.$$

$$\langle x^2 \rangle = \langle x_0^2 \rangle + 0 + 2D_0 \int_0^t \int_0^t \delta(s - \tau) ds d\tau$$

$$\langle x^2 \rangle = \langle x_0^2 \rangle + 0 + 2D_0 \int_0^t ds$$

$$\rightarrow \sigma^2 = \langle x^2 \rangle - \langle x_0^2 \rangle = 2D_0 t$$

Here, we notice that the variance is growing linearly with time, confirming the normal diffusion case, and the diffusion coefficient is given by:

$$c = \lim_{t \rightarrow \infty} \frac{\sigma^2}{2t} = D_0$$

For the anomalous diffusion, the variance takes the form $\sigma^2 = 2ct^\alpha$, with $\alpha > 1$ and $\alpha < 1$ for the super diffusion and sub-diffusion respectively. In this chapter we will study two cases dealing with normal diffusion: the unbounded and bounded diffusion; bounded diffusion usually referred to as reflected Brownian motion. By no means this would be a comprehensive study of normal diffusion but it captures the main and prominent characteristics and discuss them in more details.

A deterministic version of Eq. (4.1.1) would be the one dimensional Fokker-Planck Equation (FPE):

$$\frac{\partial u(x,t)}{\partial t} = c \frac{d^2 u(x,t)}{dx^2}$$

In addition to treat the stochastic picture, we will also study the above FPE with initial condition $u(x,0) = \delta(x)$, and two different types of boundary conditions: Neumann and Dirichlet boundary conditions.

4.2 Unbounded Free Diffusion.

Diffusion of ink molecules in water happens down the concentration gradient: ink molecules move from the region of high concentration to the region of lower concentration. Here the motion is considered over-damped and there is no explicit force driving the molecules except the random kicks from water molecules, so the FPE takes the form

$$\frac{\partial u}{\partial t} = c \frac{d^2 u}{dx^2} \quad (4.2.1)$$

on the domain $-\infty < x < \infty$. Where c is the diffusion coefficient. $x(t)$ is the position of the particle at some given time, and $u(x,t)$ represents the probability distribution function (PDF) of the particle position at given time instant t . We will study this real world problem and assume that the ink drop is initially inserted at the midway of the x -axes, i.e. at $x=0$. Thus the initial condition will be

$u(x, 0) = \delta(x)$. Using Fourier Transform (FT):

$$\hat{u}(k, t) = \int_{-\infty}^{\infty} u(x, t) e^{-ikx} dx$$

And the Inverse Fourier Transform (IFT):

$$u(x, t) = \frac{1}{2\pi} \int_{-\infty}^{\infty} \hat{u}(k, t) e^{ikx} dk$$

By applying the FT to Eq. 4.2.1 term by term, we get

$$FT\left(\frac{\partial u}{\partial t}\right) = \int_{-\infty}^{\infty} \frac{\partial u}{\partial t}(x, t) e^{-ikx} dx = \frac{\partial \hat{u}}{\partial t}, \text{ and}$$

$$FT\left(\frac{d^2 u}{dx^2}\right) = \int_{-\infty}^{\infty} \frac{d^2 u}{dx^2}(x, t) e^{-ikx} dx$$

Using integration by parts and knowing that $\lim_{x \rightarrow \pm\infty} u(x, t) = 0$; then

$$FT\left(\frac{d^2 u}{dx^2}\right) = -k^2 \int_{-\infty}^{\infty} u(x, t) e^{-ikx} dx = -k^2 \hat{u}(k, t)$$

Thus, the application of FT to eq. (4.2.1) resulting in the following differential equation:

$$\frac{\partial \hat{u}}{\partial t} = -k^2 c \hat{u}(k, t)$$

Which can be solved using the methods of ordinary differential equations to get

$$\hat{u}(k, t) = \hat{u}(k, 0) e^{-k^2 ct}$$

But $u(x, 0) = \delta(x)$ after taking the fourier transform to the initial condition we have :

$$\hat{u}(k, 0) = \widehat{\delta(x)} = \int_{-\infty}^{\infty} \delta(x) e^{-ikx} dx = 1.$$

Taking IFT and solve the integral we get:

$$u(x, t) = \frac{1}{\sqrt{4\pi ct}} \exp\left(\frac{-x^2}{4ct}\right).$$

Which is a Gaussian curve centered at the starting position $x=0$. We also notice that this solution is time dependent and expected to change in shape as a function of time. This solution shows how the concentration changes over time

(note that this is normalized concentration). The product $u(x,t)dx$ represents the probability of finding the particle within a small interval dx . Using the probability density function $u(x,t)$, one can easily find the mean and variance of the particle displacement:

With mean of x , denoted by $\langle X \rangle = E[X] = \int_{-\infty}^{\infty} x p(x) dx$ and represents the first statistical moment $M_1(x)$

$$\begin{aligned} M_1(x) &= E[X] = \int_{-\infty}^{\infty} x u(x,t) dx \\ &= \int_{-\infty}^{\infty} x u(x,t) dx = \int_{-\infty}^{\infty} x \frac{1}{\sqrt{4\pi ct}} \exp\left(\frac{-x^2}{4ct}\right) dx \\ &= \frac{1}{\sqrt{4\pi ct}} \int_{-\infty}^{\infty} x \exp\left(\frac{-x^2}{4ct}\right) dx \end{aligned}$$

This is the integral of a product of odd and even functions over a symmetric integration interval, thus $M_1(x) = 0$.

To find the second moment (variance), we need to do the following

$$M_2(x) = \text{Var}[x] = \sigma^2 = E[(x - E[X])^2] = \int_{-\infty}^{\infty} x^2 u(x,t) dx.$$

$$\begin{aligned} &= \int_{-\infty}^{\infty} x^2 \frac{1}{\sqrt{4\pi ct}} \exp\left(\frac{-x^2}{4ct}\right) dx \\ &= \int_{-\infty}^{\infty} x^2 \frac{1}{\sqrt{4\pi ct}} \exp\left(\frac{-x^2}{4ct}\right) dx \\ &= \frac{1}{\sqrt{4\pi ct}} \int_{-\infty}^{\infty} x^2 \exp\left(\frac{-x^2}{4ct}\right) dx, \text{ using integration by parts, we get} \end{aligned}$$

$$\sigma^2 = 2 c t,$$

A result we have found using the Langevin equation (LE) Eq. 4.1.1 in the previous section. This verifies that both pictures, the stochastic and the FPE approaches renders the same final results, though the formulation is different: the former is stochastic in nature and give more information on the dynamic of the particle, and the later is deterministic which treats the distribution of the particle's position.

Now, we turn another time to LE and we will solve it using Euler-Maryuma method [28]. To solve eq. 4.1.1 numerically, we use Matlab code to integrate the Stochastic differential equation (SDE) with time step k , with the initial condition $x_0=0$, noise intensity D_0 , and number of realization (number of particles) M . The integration is carried out till a certain value of the time given by t_{max} . a typical step by step algorithm for the Matlab code is shown below:

1- choose appropriate D_0 (noise intensity), k , t_{max} , $N = (t_{max}/k)$.

2- generate a Gaussian random (η_i) number using the matlab function `randn`

3- choose a large number of particle such that $M = 10^4$ particles .

4- use the following update rule for the particle position [15]

$$x_{i+1} = x_i + \sqrt{2D_0k} \eta_i$$

The above algorithm generates a time trajectory for every particle of the M particles. These trajectories are noisy due to the inherited randomness coming from the random force term. Figure 4.2.1 shows the trajectories for few of these particles. We notice that as time progress the particles spend most of the time around the zero position and some rarely go away from it, indicating that the probability of finding the particle around the zero is higher than other places. This agrees with our calculations of the mean of the particle's position in the previous section. Another way to quantify this is to find the variance, a measure which quantifies how far the particle move away from the mean, or deviates from the mean value. As derived before, the deviation grows linearly with time, indicating that as the time pass by, there is a higher chance to find the particle away from the starting point which is $x_0=0$ as compared to the distribution at earlier time. Thus, as the time $t \rightarrow \infty$, the particle, on average move away from the starting point.

Since, approaching an infinite time is computationally not feasible, one can rely on the principles of statistics and generate an ensemble of these trajectories, each with length t_{\max} . To do so, the process should satisfy the ergodicity condition. A process is ergodic if the time averaged mean square displacement (TAMSD) is equal to the ensemble averaged mean square displacement (EAMSD).

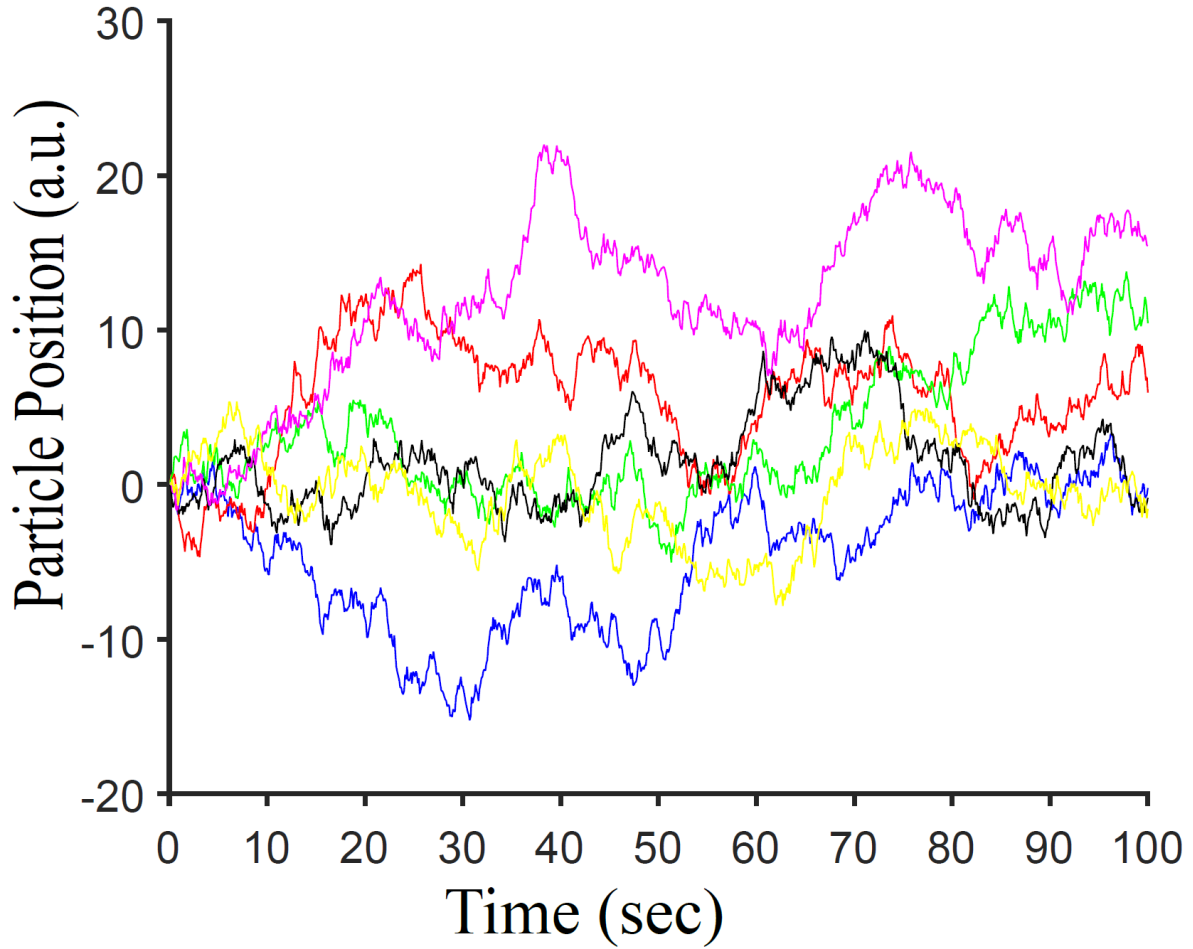


Figure (4.2.1): Time traces for unbounded diffusing Brownian particles. The particles are independent. The curves are generated using time step $k=0.1$ sec., and noise intensity $D_0=1$. The particle position is given in arbitrary length units.

The time series $x(t')$ of length t (the measurement time) is thus evaluated in terms of squared differences of the particle position separated by the so-called lag time Δ which defines the width of the window slid along the time series $x(t')$. Typically $\overline{(\delta^2(\Delta; t))}$ is considered in the limit $\Delta \ll t$ to obtain good statistics. Thus, we calculated TAMSD, for each particle, using [31; 34]

$$\overline{(\delta^2(\Delta, t))} = \frac{1}{t - \Delta} \int_0^{t-\Delta} (x(\dot{t} + \Delta) - x(\dot{t}))^2 d\dot{t}.$$

Where t is the total time and here $t = t_{\max}$. The EAMSD or shortly referred to as MSD is calculated simply by generating an ensemble of M realization, and calculated the variance at each instant of time t

$$\text{MSD} = \langle (x(t) - x_0)^2 \rangle$$

Our results showed deviation between the TAMSD and EAMSD for large time lags. But when we used the ensemble average of the TAMSD, the two definitions give the same result as shown in figure 2. This indicates that the Brownian motion considered above is ergodic. Thus, it is sufficient to use the ensemble average. Using the EAMSD allows us to run the simulation for short time but for large number of particles, rendering a short running time in Matlab.

Figure (4.2.2) shows that the variance grows linearly with time as expected and so it can be fitted with $\sigma^2 = 2 c t$, where c is the diffusion coefficient which can be evaluated from the time series by dividing $(\overline{\delta^2(\Delta, t_{\max})})$ by 2Δ , in the limit $t_{\max} \rightarrow \infty$. The fit is also plotted in figure 4.2.2 but shifted by hand below for clarity. From the fit one can see that the diffusion coefficient is $c=1$, and $\alpha =1$ corresponding to normal diffusion case.

In our case, the diffusion is free normal diffusion and from the FPE we expect to have a Gaussian function for the probability density. Indeed, by dividing the x-axis to n consecutive intervals, and counting the number of particles whose position fall within each one these intervals, we generated a histogram and

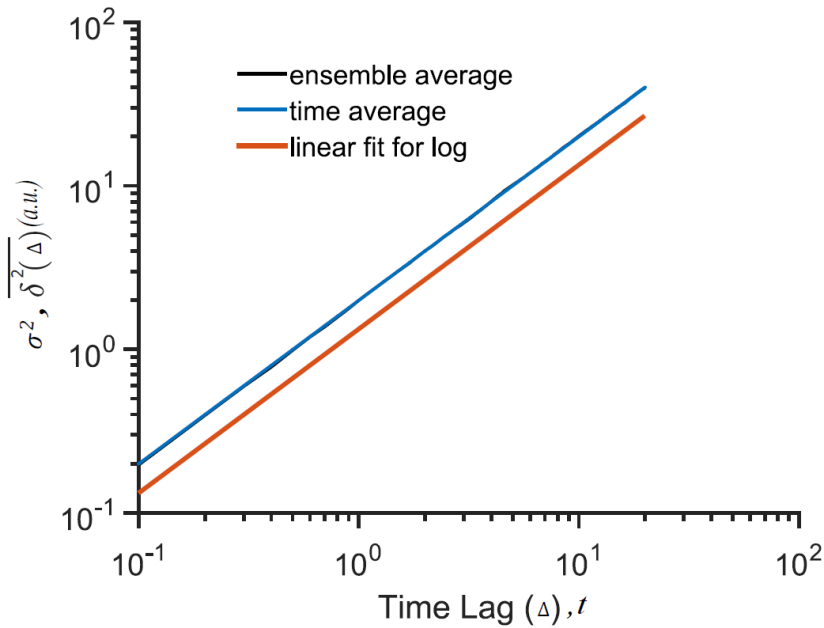


Figure (4.2.2): Mean square displacement for Brownian particle, generated using 10^4 particle realizations, for different values of time lag (Δ). Blue curve represent an ensemble average of the time averaged mean square displacement plotted versus the time t , Black line underneath the blue line represent the ensemble averaged mean square displacement. Red line is the linear fit of the data in the blue line, it is shifted downward for clarity. The simulation was carried out with time step $k=0.1$ sec, and noise intensity of $c=1$.

normalize it to the total number of particles we get a bell shaped histogram as shown in figure (4.2.3). Figure (4.2.3) shows this histogram fitted with the solution for FPE at three distinct time instants. We notice that the bell shape is preserved, but the width and the height of the curve is changing with time. As time increases, the height of the peak is reduced and the width spread. i.e. the PDF of the particle decreases exponentially. After an infinitely long time the probability of finding the particle near the origin approaches to zero as shown in figure (4.2.4). The spreading of the bell curve is a signature for the changing in the variance which we showed it grows linearly. Strictly speaking the full width half maxima which is defined by the points on the x-axis corresponding to

maximum value divided by 2 is 2.35σ . Moreover, we notice that the particles didn't drift and the peak remain at zero. A valid result from the setup of the free Brownian motion problem with no drift.

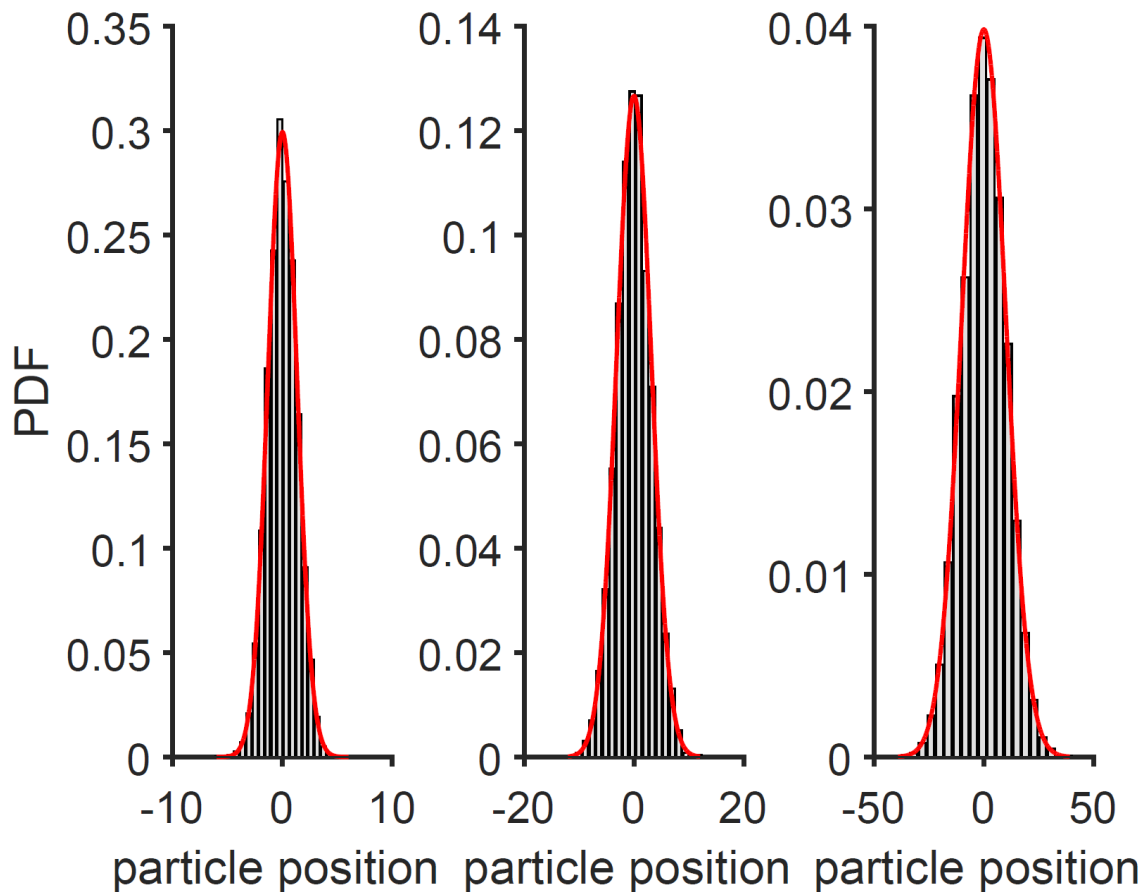


Figure (4.2.3): Normalized probability distribution function (PDF) at three instants of time $t=1, 5$ and 50 sec. The bars represent the normalized number of particles within a bin width. The red line is generated using analytical formula for the PDF. The simulation was carried out with noise intensity $D_0=1$, time step $k=0.1$ sec for 10^4 particles.

So, in this case in order to give a more comprehensive vision about this distribution for the Brownian motion increments, we have plotted with a simple script in Matlab, different probability distribution functions for the Brownian

motion which showed a normal distribution with zero mean and variance that is increasing with time.

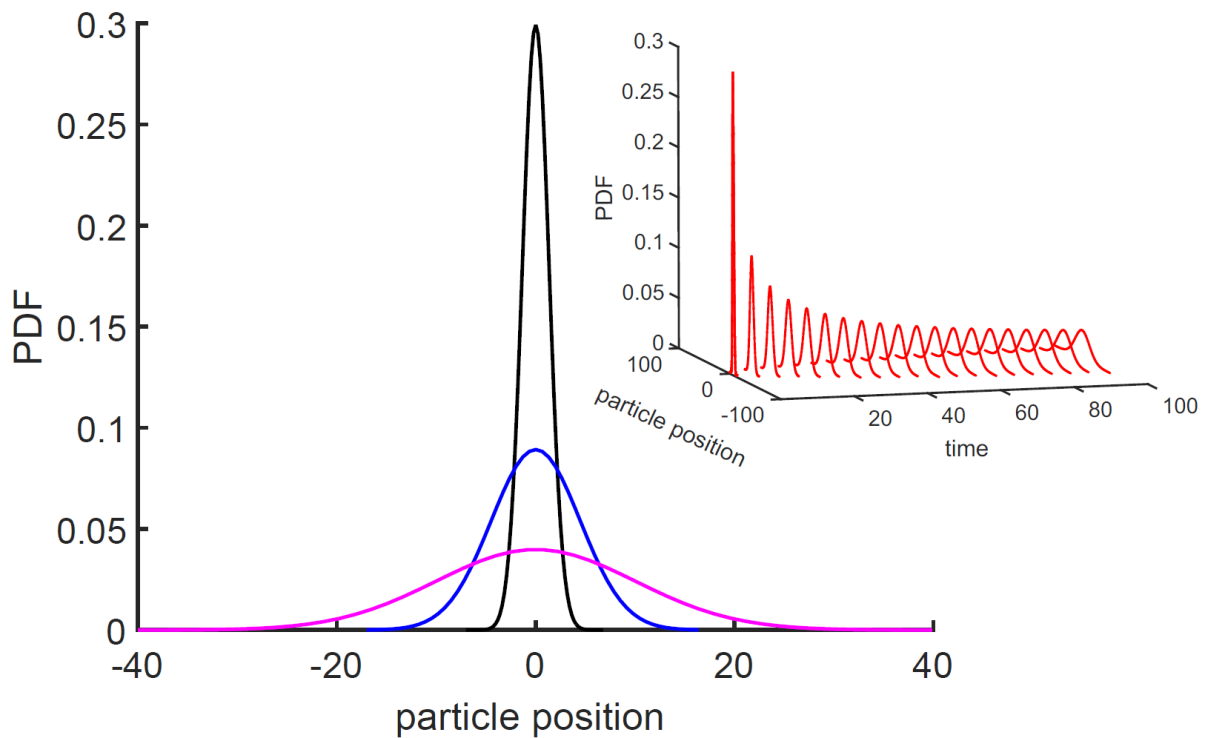


Figure (4.2.4): Normalized PDF of the particle position (in arbitrary units) for three instants of time $t = 1$, 5 , and 50 seconds. The inset shows how the PDF changes every four seconds. The curves are generated using the analytical formula for the PDF.

4.3 Bounded Free Brownian Motion.

Unbounded diffusion is an idealization for many real-world problems and in some cases the space available for the particle to diffuse is much larger than most expected spatial step size. But this is not the case when it comes to proteins diffusing within the cell or the cell membrane [41]. Various

experiments in biology and semiconductor physics reported on the appearance of reflected Brownian behavior [12; 33], and some reported a change in the time rate at which the particle's position variance grows in bounded setups.

Here we treat bounded diffusion and discuss the effect of the boundaries on the analytical and numerical solutions. We will use point source as initial condition, and restrict the particle to move in the interval $x \in [0, 1]$; without loss of generality our analysis will be applicable to the interval $[0, L]$. Here, we impose Neumann boundary conditions where there will be no net flux of the particles at the boundaries, that is

$$\frac{\partial u(x,t)}{\partial x} \Big|_{x=0} = \frac{\partial u(x,t)}{\partial x} \Big|_{x=L} = 0$$

Considering the initial condition

$$U(x, 0) = \delta(x - 0.4).$$

with the above initial and boundary conditions the solution of Eq. 4.2.1 can be written using the separation of variables technique [11]

$$U(x,t) = \frac{1}{L} + \frac{2}{L} \sum_{n=1}^{\infty} \left\{ e^{-\left(\frac{n\pi}{2}\right)^2 \frac{t-t_0}{\tau}} \cos\left(\frac{n\pi x}{L}\right) \cos\left(\frac{n\pi x_0}{L}\right) \right\} \quad (4.3.1)$$

Where the characteristic time-scale $\tau = \frac{\left(\frac{L}{2}\right)^2}{D_0}$ and t_0 is the starting time which is

zero in our computations. Alternatively, the solution can be written as

$$u(x, t) = \frac{1}{2\sqrt{\pi D_0 t}} \sum_{n=-\infty}^{n=+\infty} \left\{ e^{-\frac{(x-x_0+2nL)^2}{4D_0 t}} + e^{-\frac{(x+x_0+2nL)^2}{4D_0 t}} \right\} \quad (4.3.2)$$

With $x_0 = 0.4$, and $L=1$ in our case. The former solution converges rapidly at large t while the second converges rapidly at small values of t .

Monte Carlo simulation is used where Euler-Maruyama method was implemented in a similar manner of the previous case, but with modifications concerning the boundary conditions. The following algorithm was followed step by step in the simulation

1- choose appropriate D_0 (noise intensity), k , t_{max} , $N = (t_{max} / k)$.

2- generate a Gaussian random (η_i) number using the Matlab function `randn`

3- choose a large number of particle such that $M = 10^4$ particles .

4- use the following update rule for the particle position

$$x_{i+1} = x_i + \sqrt{2D_0 k} \eta_i$$

5- if $x_{i+1} < 0$, then $x_{i+1} = -x_{i+1}$

6- if $x_{i+1} > L$, then $x_{i+1} = 2L - x_{i+1}$

The last two steps of the algorithm are to ensure specular reflection of the particle when it hits the boundaries. Different scenarios are considered for this type of reflection, but we followed [15]. The simulation was run for 5000 realizations each with 20 minutes length, with noise intensity $D_0=0.001$ and

time step $k=0.1$ sec. Figure (4.3.1) shows several particle trajectories, we see that when the particle diffuses and hits either boundaries at $x=0$ and $L=1$, the particle is reflected instantaneously as imposed by step 5 and 6 in the algorithm. After reflection the particle continues its Brownian behavior which results in noisy time traces as illustrated in figure (4.3.1). When comparing these traces with figure (4.2.1), clearly we notice the effect of the boundaries which make the trajectory have turning points affecting the direction of the motion for the next few time steps.

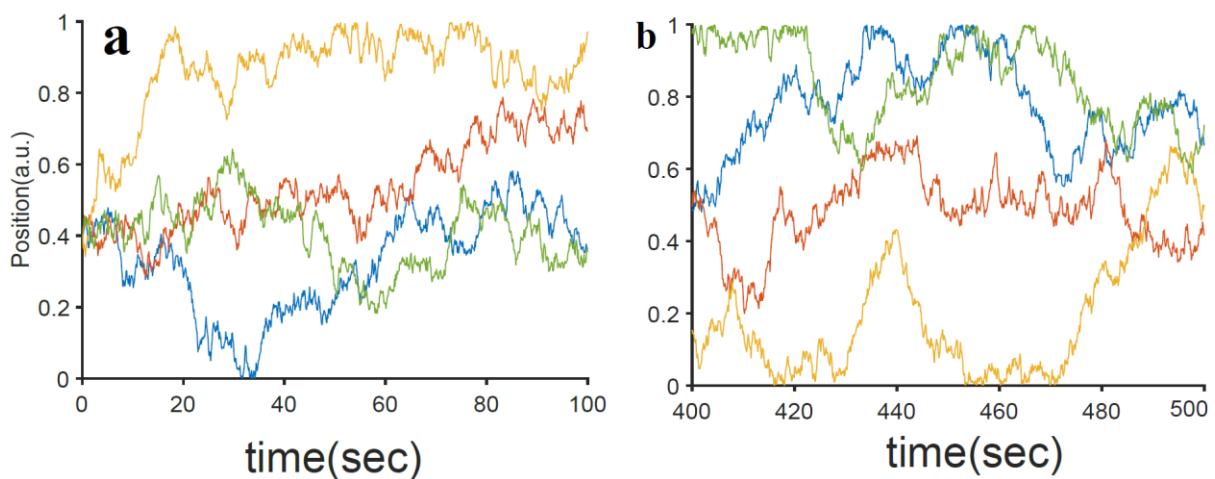


Figure (4.3.1): Time traces for bounded diffusing Brownian particles. The particles are independent. The curves are generated using time step $k=0.1$ sec., and noise intensity $D_0=0.001$. The particle position is given in arbitrary length units. panel (a) shows the trajectories for short time, while panel (b) shows the same trajectories but for large times

The effect becomes more dominant for larger times $t > \tau$ causing a disturbance and deviation from free Brownian motion: For small times (see figure(4.3.1-a)) and small spatial random step sizes, the particle harboring around the starting point, as the time pass, intuitively the particle will approaches the boundaries (see figure (4.3.1-b)) which is verified by the linear increase of the variance as

shown in figure (4.3.2). But upon approaching the boundaries the particle is forced to change direction, this change in the direction is observed in the trajectories and accompanied by a decrease in the rate at which the variance grows, the process continues and for large times $t \gg \tau$ the rate at which the variance grows becomes zero, which is indicated by the flat region in figure (4.3.2).

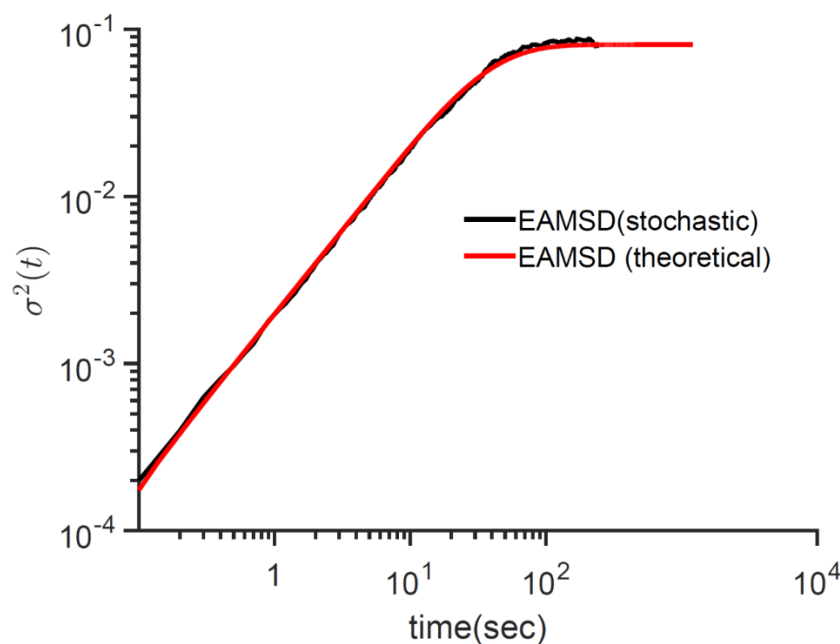


Figure (4.3.2): MSD of reflected Brownian motion in the interval $[0,1]$. The black line represent the MSD calculated from the stochastic Langevin equation, using 1000 realization, $k=0.1$ sec, and noise intensity of $D_0=0.001$. Red line, is the same quantity but generated using the distributions in eq. 4.3.1 and eq. 4.3.2

To characterize this phenomenon further, we plotted the PDF using Eq. 4.3.1 and Eq. 4.3.2 and found that the PDF which is the solution $u(x,t)$ for the FPE (see Fig. 4.3.4) and showed that for small times the curves look Gaussian in shape which agrees with the free diffusion case. For intermediate times (Fig. 4.3.3 green line, and Fig. 4.3.4 middle panel), the curves become less symmetric

and have non-zero value at $x=0$, indicating that more particles are located to the right of the origin as compared to number accumulated to the left of L . The accumulation of the particles near one boundary increase the chances of hitting the boundary and be reflected. Thus make the distribution is biased, resulting in deviation of the variance from the linear relation with time as shown Fig. 4.3.2.

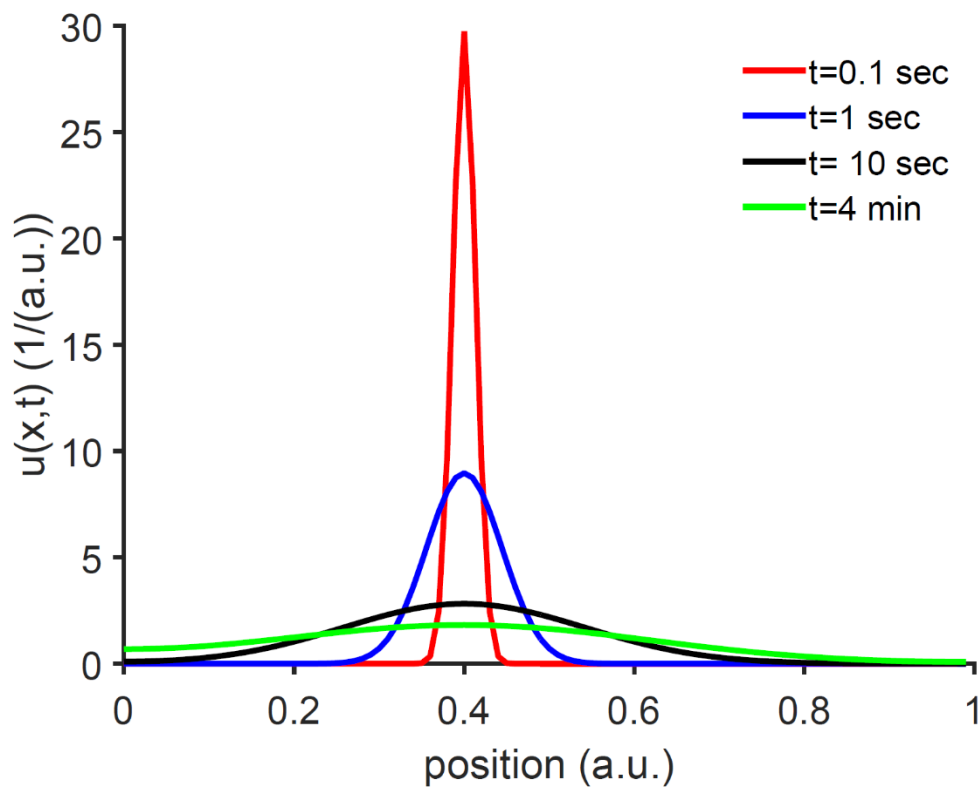


Figure (4.3.3): Different solutions of the FPE for the reflected Brownian motion using Eq. 4.3.1 and 4.3.2. The solutions are at different times as indicated in legend. We used 50 terms for the series in Eq. 4.3.1 and 100 terms for the series in Eq. 4.3.2

For large times, the PDF has the value of 1, with a nearly uniform distribution over the interval L , with a variance saturates to the value of $1/12$ as that expected for uniform distribution, $P(x)=1/L$, whose variance is given by $L^2/12$, in our case the length of the interval is $L=1$.

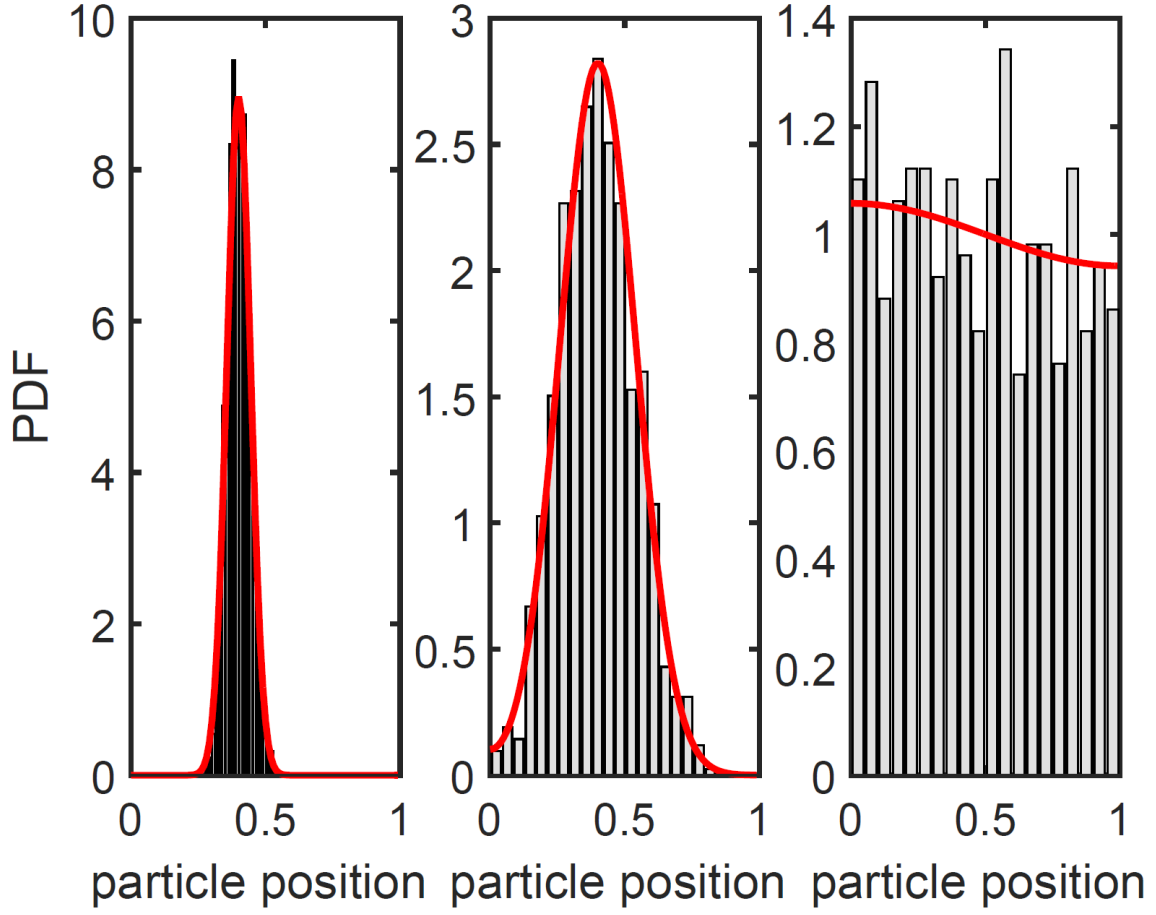


Figure (4.3.4): Probability distribution function for the bounded diffusion case generated using the histogram method in Matlab, the simulation was run for the parameter values; $k=0.1$ sec, $D_0=0.001$, and 1000 particles. The red line represent the PDF generated using a code combining Eq. 4.3.1 and 4.3.2 based on the convergence speed. We used 50 terms for the series in Eq. 4.3.1 and 100 terms for Eq. 4.3.2

To characterize the slowness of the diffusion, we calculated the value of α , where as noted earlier, the variance grows as $\sigma^2 = 2ct^\alpha$. To do so, α was calculated as

$$\alpha = \frac{d \log(\sigma^2)}{d \log(t)}$$

We used the variance calculated using the ensemble average generated using Eq. 4.3.1 and Eq. 4.3.2 rather than using the variance from the stochastic

stimulation although in theory it should give the same result, but the curve is not smooth as that generated using the distributions in Eq. 4.3.1 and 4.3.2

Figure 4.3.5, shows that α stays constant ($\alpha = 1$) for short time, then starts decreasing till it reaches to zero nearly after 200 seconds. This is another way to see that, the boundaries result in slower diffusion; an effect that is reported as transient fractional behavior in specific experimental setups [16; 41] and showed here in a generic setup.

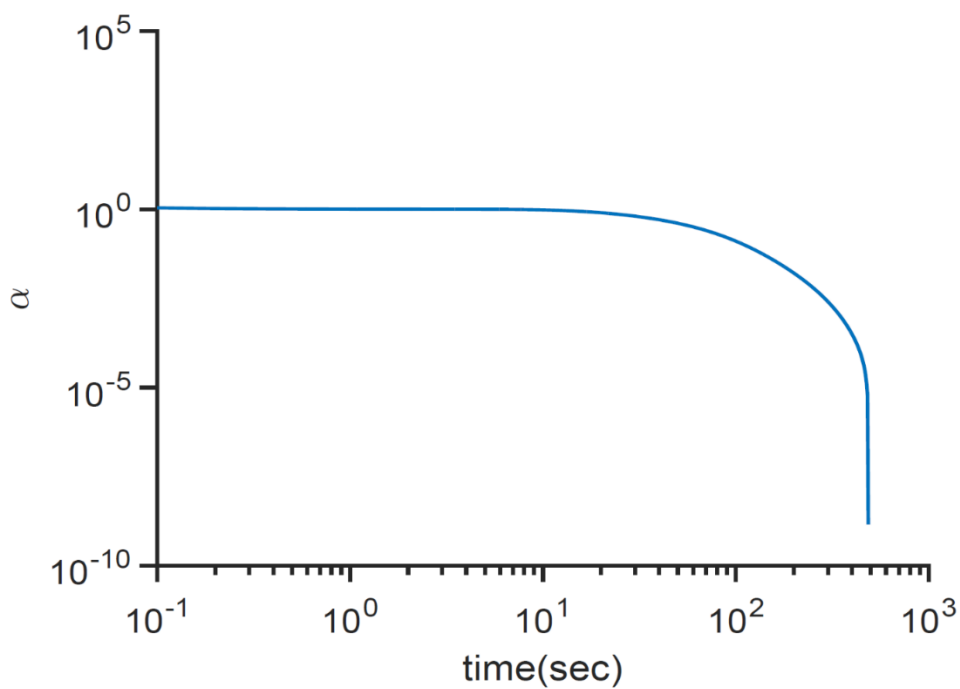


Figure (4.3.5): Calculated values of alpha using the data plotted by the red line in fig. 4.3.2. The derivative is taken numerically using Matlab code.

Conclusion and Outlook

In this thesis, we discussed the solution of Fokker–Planck equation, Firstly, we talked about the exact solution using separation of variables for fractional Fokker –Planck equation, using Caputo derivative for fractional case. Also, we discussed the existence and the uniqueness of the solution. In particular, we presented the analytical solution in sections 2.2, and 2.4 in more details as compared to previous books and periodicals. Secondly, we talked about the numerical solution of Fokker-Planck equation using explicit finite difference. Finally, we proved the stability of solution in both cases ordinary and fractional, especially, we investigated the stability in section 2.3, which was not discussed in the previous books and periodicals.

In the last chapter, we found the solution for the FPE within two setups and using two different methods, yet they describe the same Phenomenon. The cases that are considered are the unbounded and the bounded diffusion, while, the two approaches are: the analytical solution of FPE with the aforementioned setups, and the stochastic simulation. FPE shows how the width of the distribution changes over time, while the stochastic method dives deeper, and shows how the particles spread from the starting initial condition. Moreover, the second case shows how confining the free diffusing particle results in a transient fractional behavior.

In the light of recent advances both in stochastic and fractional calculus, where researchers use pre-assumed distributions for the space and time steps taken by the particle and simulate the fractional behavior. We suggest to use more realistic obstacles extracted from experimentally recorded time series. This will allow us to study FPE with different values of α and β that has real-world significance.

References

- 1- Amro, R. M., Lindner, B., & Neiman, A. B. (2015). Phase diffusion in unequally noisy coupled oscillators. *Physical review letters*, 115(3), 034101.
- 2- Amro, R. M., & Neiman, A. B. (2014). Effect of voltage oscillations on response properties in a model of sensory hair cell. Paper presented at the International Conference on Theory and Application in Nonlinear Dynamics (ICAND 2012).
- 3- Asmar, N. H. (2016). *Partial differential equations with Fourier series and boundary value problems*: Courier Dover Publications.
- 4- Berg-Sørensen, K., & Flyvbjerg, H. (2005). The colour of thermal noise in classical Brownian motion: a feasibility study of direct experimental observation. *New Journal of Physics*, 7(1), 38.
- 5- Berry, H., & Chaté, H. J. P. R. E. (2014). Anomalous diffusion due to hindering by mobile obstacles undergoing Brownian motion or Orstein-Uhlenbeck processes. 89(2), 022708.
- 6- Bickel, T. (2007). A note on confined diffusion. *Physica A: Statistical Mechanics and its Applications*, 377(1), 24-32.
- 7- Bonani, F., & Ghione, G. (2001). Noise in semiconductor devices. In *Noise in Semiconductor Devices* (pp. 1-38): Springer.
- 8- Boyce, W. E., DiPrima, R. C., & Meade, D. B. (2017). *Elementary differential equations*: John Wiley & Sons.
- 9- Brannan, J. R., & Boyce, W. E. (2015). *Differential equations: An introduction to modern methods and applications*: John Wiley & Sons.
- 10- Bressloff, P. C., & Newby, J. M. (2013). Stochastic models of intracellular transport. *Reviews of Modern Physics*, 85(1), 135.
- 11- Carslaw, H. S., & Jaeger, J. C. (1959). *Conduction of heat in solids* (No. 536.23). Clarendon Press.
- 12- Choo, K., Muniandy, S., Woon, K., Gan, M., & Ong, D. (2017). Modeling anomalous charge carrier transport in disordered organic semiconductors using the fractional drift-diffusion equation. *Organic Electronics*, 41, 157-165.

- 13- de Grooth, B. G. (1999). A simple model for Brownian motion leading to the Langevin equation. *American journal of physics*, 67(12), 1248-1252.
- 14- Dos Santos, M. A. (2018). Non-Gaussian distributions to random walk in the context of memory kernels. *Fractal and Fractional*, 2(3), 20.
- 15- Erban, R., Chapman, J., & Maini, P. (2007). A practical guide to stochastic simulations of reaction-diffusion processes. arXiv preprint arXiv:0704.1908.
- 16- Ernst, M., John, T., Guenther, M., Wagner, C., Schaefer, U. F., & Lehr, C. M. (2017). A model for the transient subdiffusive behavior of particles in mucus. *Biophysical journal*, 112(1), 172-179.
- 17- Evangelista, L. R., & Lenzi, E. K. (2018). *Fractional diffusion equations and anomalous diffusion*: Cambridge University Press.
- 18- Ezzat, M. A., El-Karamany, A. S., & Fayik, M. A. (2012). Fractional ultrafast laser-induced thermo-elastic behavior in metal films. *Journal of Thermal Stresses*, 35(7), 637-651.
- 19- Falasco, G., Gnann, M. V., Rings, D., & Kroy, K. (2014). Effective temperatures of hot Brownian motion. *Physical Review E*, 90(3), 032131.
- 20- Frey, E., & Kroy, K. (2005). Brownian motion: a paradigm of soft matter and biological physics. *Annalen der Physik*, 14(1-3), 20-50.
- 21- Gammaitoni, L., Hänggi, P., Jung, P., & Marchesoni, F. (1998). Stochastic resonance. *Reviews of modern physics*, 70(1), 223.
- 22- Genthon, A. (2020). The concept of velocity in the history of brownian motion. *The European Physical Journal H*, 45(1), 49-105.
- 23- Gómez-Aguilar, F., & Alvarado-Méndez, E. (2015). Description of the dynamics of charged particles in electric fields: an approach using fractional calculus. In *Advanced lasers* (pp. 147-158): Springer.
- 24- Gorenflo, R., Kilbas, A. A., Mainardi, F., & Rogosin, S. V. (2014). *Mittag-Leffler functions, related topics and applications* (Vol. 2): Springer.
- 25- Goychuk, I., Kharchenko, V. O., & Metzler, R. (2014). Molecular motors pulling cargos in the viscoelastic cytosol: how power strokes beat subdiffusion. *Physical Chemistry Chemical Physics*, 16(31), 16524-16535.

- 26- Hanna, J. R., & Rowland, J. H. (2008). Fourier series, transforms, and boundary value problems: Courier Corporation.
- 27- Herzel, H. (1991). Risken, H., The Fokker-Planck-Equation. Methods of Solution and Applications. Berlin etc., Springer-Verlag 1989. XIV, 472 pp., 95 figs., DM 98,—. ISBN3-540-50498-2 (Springer Series in Synergetics 18).
- 28- Higham, D. J. (2001). An algorithmic introduction to numerical simulation of stochastic differential equations. SIAM review, 43(3), 525-546.
- 29- Hilfer, R. (Ed.). (2000). Applications of fractional calculus in physics. World scientific.
- 30- Hoffman, J. D., & Frankel, S. (2018). Numerical methods for engineers and scientists: CRC press.
- 31- Huang, F., Watson, E., Dempsey, C., & Suh, J. (2013). Real-time particle tracking for studying intracellular trafficking of pharmaceutical nanocarriers. In Cellular and Subcellular Nanotechnology (pp. 211-223): Springer.
- 32- Jeon, J. H., Leijnse, N., Oddershede, L. B., & Metzler, R. (2013). Anomalous diffusion and power-law relaxation of the time averaged mean squared displacement in worm-like micellar solutions. New Journal of Physics, 15(4), 045011.
- 33- Kalwarczyk, T., Kwapiszewska, K., Szczepanski, K., Sozanski, K., Szymanski, J., Michalska, B., . . . Holyst, R. (2017). Apparent anomalous diffusion in the cytoplasm of human cells: the effect of probes' polydispersity. The Journal of Physical Chemistry B, 121(42), 9831-9837.
- 34- Kepten, E., Weron, A., Sikora, G., Burnecki, K., & Garini, Y. (2015). Guidelines for the fitting of anomalous diffusion mean square displacement graphs from single particle tracking experiments. PLoS One, 10(2), e0117722.
- 35- Kilbas, A. A., Srivastava, H. M., & Trujillo, J. J. (2006). Theory and applications of fractional differential equations (Vol. 204): elsevier.
- 36- Lindner, Benjamin. "The diffusion coefficient of nonlinear Brownian motion." New Journal of Physics 9.5 (2007): 136.
- 37- Meerschaert, M. M., & Sikorskii, A. (2019). Stochastic models for fractional calculus: de Gruyter.

- 38- Meerschaert, M. M. (2012). Fractional calculus, anomalous diffusion, and probability. *Fractional dynamics: recent advances*, 265-284.
- 39- Metzler, R., Jeon, J. H., Cherstvy, A. G., & Barkai, E. (2014). Anomalous diffusion models and their properties: non-stationarity, non-ergodicity, and ageing at the centenary of single particle tracking. *Physical Chemistry Chemical Physics*, 16(44), 24128-24164.
- 40- Metzler, R., & Klafter, J. (2000). The random walk's guide to anomalous diffusion: a fractional dynamics approach. *Physics reports*, 339(1), 1-77.
- 41- Mortensen, K. I., Flyvbjerg, H., & Pedersen, J. N. (2021). Confined Brownian motion tracked with motion blur: Estimating diffusion coefficient and size of confining space. *Frontiers in Physics*, 8, 601.
- 42- Mustapha, K., Abdallah, B., & Furati, K. M. (2014). A discontinuous Petrov--Galerkin method for time-fractional diffusion equations. *SIAM Journal on Numerical Analysis*, 52(5), 2512-2529.
- 43- Mustapha, K., & AlMutawa, J. (2012). A finite difference method for an anomalous sub-diffusion equation, theory and applications. *Numerical Algorithms*, 61(4), 525-543.
- 44- Myint-U, T., & Debnath, L. (2007). *Linear partial differential equations for scientists and engineers*. Springer Science & Business Media.
- 45- Nelson, B. (2019). *The Weierstrass Function*. Retrieved December, 31.
- 46- Pavliotis, G. A. (2009). *Applied stochastic processes*. Lecture Notes, Pre-Print.
- 47- Peters, O. (2019). The ergodicity problem in economics. *Nature Physics*, 15(12), 1216-1221.
- 48- Podlubny, I. (1998). *Fractional differential equations: an introduction to fractional derivatives, fractional differential equations, to methods of their solution and some of their applications*: Elsevier.
- 49- Radpay, P. (2020). *Langevin Equation and Fokker-Planck Equation*.
- 50- Regner, B. M., Vučinić, D., Domnisoru, C., Bartol, T. M., Hetzer, M. W., Tartakovsky, D. M., & Sejnowski, T. J. (2013). Anomalous diffusion of single particles in cytoplasm. *Biophysical journal*, 104(8), 1652-1660.
- 51- Rolski, T., Schmidli, H., Schmidt, V., & Teugels, J. L. (2009). *Stochastic processes for insurance and finance (Vol. 505)*: John Wiley & Sons.

- 52- Sebah, P., & Gourdon, X. (2002). Introduction to the gamma function. *American Journal of Scientific Research*, 2-18.
- 53- Sharma, S. (2005). Brownian motion problem: Random walk and beyond. *Resonance*, 10(8), 49-66.
- 54- Stirzaker, D. (2005). *Stochastic processes and models*. OUP Catalogue.
- 55- Szabados, T. (2010). An elementary introduction to the Wiener process and stochastic integrals. arXiv preprint arXiv:1008.1510.
- 56- Bromwich, T. J. (1991). I'A. and MacRobert, TM *An Introduction to the Theory of Infinite Series*.
- 57- Uhlenbeck, G. E., & Ornstein, L. S. (1930). On the theory of the Brownian motion. *Physical review*, 36(5), 823.
- 58- Yuste, S. B., & Acedo, L. (2005). An explicit finite difference method and a new von Neumann-type stability analysis for fractional diffusion equations. *SIAM Journal on Numerical Analysis*, 42(5), 1862-1874.